NTNU – Trondheim
Norwegian University of
Science and Technology

Analysis Methods for Mooring Systems with focus on Accidental Limit State

Lars Christian Stendal

Marine Technology
Submission date: June 2015
Supervisor: Kjell Larsen, IMT

Norwegian University of Science and Technology
Department of Marine Technology

NTNU Trondheim
Norges teknisk-naturvitenskapelige universitet
Institutt for marin teknikk

MASTER THESIS SPRING 2015

for

Stud. tech. Lars Christian Stendal

Analysis Methods for Mooring Systems with focus on Accidental Limit State

Analyse av forankringssystemer – fokus på analyse og konsekvens av linebrudd

Background

The purpose of the mooring system is to keep a floating vessel safely at a required position. It normally consists of 8-16 mooring lines of heavy chain, steel wire ropes and/or synthetic polyester ropes connected to a seabed anchor.

During the past years, the requirements to the mooring and station keeping systems of mobile and permanent units have become more complex;
- The industry is moving into new frontiers (ultra-deep water down to 3000m depth and into arctic areas).
- There are more operations adjacent to other installations (flotel operations and tender support vessel operations).
- The new mobile units are becoming larger and many units are at the end of their lifetime.

In addition, mooring failure rate is unacceptably high. Some incidents have been multiple line failures, leading to vessel drifting. The investigations show a variety of direct causes covering both inaccurate design, bad quality on mooring line components and lack of personnel competence related to operation of the system.

This master thesis shall build on the work performed during the project work carried out autumn 2014.

The response quantities to be studied comprise extreme motions (offset) of the floating vessel and extreme tensions in the most loaded mooring lines. Acceptable design is controlled by check of the ultimate limit state (ULS) and accidental limit state (ALS) design criteria. Focus of this thesis shall be on the load effect part of the design (not the resistance/capacity).

Analysis methods for estimating ultimate mooring line tension and vessel offset can be divided into frequency domain (FD) methods and time domain (TD) methods. Using FD methods, the low frequency (LF) load effects and the wave frequency (WF) load effects are analysed separately and then combined into characteristic values used in recipes for ULS and ALS design. The dynamic system describing the behavior of the vessel must be linearized and the maxima of vessel motions and line tensions are usually assumed to be statistically distributed according to the Rayleigh distribution. Sometimes empirical corrections for non-Rayleigh distributions are, however, performed. When using TD methods, all non-linearities

in the dynamic system (stiffness and damping) and in the excitation may be taken into account. The result of TD simulations are time series of selected responses that must be carefully analysed by relevant statistical methods in order to establish a reliable estimate of the characteristic load effect.

Scope of Work

1) a) Describe the selected vessel (Snorre B semisubmersible) in terms of main particulars, general layout and hydrodynamic properties. The description shall cover characteristics of wind forces, current forces, wave drift forces and first order motion RAOs.
b) Describe the ULS and ALS acceptance criteria (safety factors and recipes) relevant for the Norwegian Continental Shelf (NCS).

2) Review relevant literature and describe the different aspects and differences of FD and TD analysis methods for analysis of extreme vessel offset and extreme mooring line tension based on the short term storm approach. The software tools MIMOSA (FD) and SIMO/RIFLEX (TD) shall be used. Base case method for TD shall be the fully coupled approach.

3) Establish numerical simulation models for TD and FD analysis. Select the two water depths, mooring systems and metocean design basis studied during the project work. Establish characteristic vessel offset and mooring line tensions according to recipes in rules and regulations. Make a thorough comparison of the FD and TD results. The comparison shall cover both mean, LF and WF responses as well as the total response.

4) Particular analysis of a line failure in a selected storm. As a background, a brief review of mooring line failures experienced shall be reported based on 2-3 available publications. In view of industry experience, it is of interest to assess if a line failure (due to overload) in a particular storm will lead to a progressive collapse of the complete mooring system. In this activity, only TD analysis shall be carried out (coupled analysis). The probability distribution of the most loaded remaining line shall be established given a failure of the neighboring line. The approach and selected case for this task shall be agreed upon with the supervisor.

5) Conclusions and recommendations for further work.

General information
All necessary input data is assumed to be provided by Statoil.

The work scope may prove to be larger than initially anticipated. Subject to approval from the supervisor, topics may be reduced in extent.

In the thesis, the candidate shall present his personal contribution to the resolution of problems within the scope of the thesis work

Theories and conclusions should be based on mathematical derivations and/or logic reasoning identifying the various steps in the deduction.

The candidate should utilise the existing possibilities for obtaining relevant literature.

Thesis format

The thesis should be organised in a rational manner to give a clear exposition of results, assessments, and conclusions. The text should be brief and to the point, with a clear language. Telegraphic language should be avoided.

The thesis shall contain the following elements: A text defining the scope, preface, list of contents, summary, main body of thesis, conclusions with recommendations for further work, list of symbols and acronyms, references and (optional) appendices. All figures, tables and equations shall be numerated.

The supervisor may require that the candidate, in an early stage of the work, presents a written plan for the completion of the work.

The original contribution of the candidate and material taken from other sources shall be clearly defined. Work from other sources shall be properly referenced using an acknowledged referencing system.

The report shall be submitted in two copies:

- Signed by the candidate
- The text defining the scope included
- In bound volume(s)
- Drawings and/or computer prints which cannot be bound should be organised in a separate folder.

Ownership

NTNU has according to the present rules the ownership of the thesis. Any use of the thesis has to be approved by NTNU (or external partner when this applies). The department has the right to use the thesis as if the work was carried out by a NTNU employee, if nothing else has been agreed in advance.

Thesis supervisor**:**

Prof. II Kjell Larsen (Statoil/NTNU)

Deadline: June 10, 2015

Trondheim, January 2015

Kjell Larsen (date and signature): Jan 28th 2015 Kjell Larsen

Lars Christian Stendal (date and signature): January 25th Lars C. Stendal

Abstract

During the last years, the oil and gas industry has moved into new frontiers, which require more complex mooring solutions. The failure rate is unacceptably high, with 43 incidents for the Norwegian Continental Shelf alone, between 2000 and 2013. It is therefore interesting to compare the mooring system design tools used by the industry, and to investigate the behaviour of a damaged mooring system.

The focus has been split between a comparison of mooring analysis in time domain and frequency domain, and an investigation of an accidental limit state(ALS) mooring analysis. The goal of the comparison was to understand the theory behind both methods, to verify, adopt, and simplify numerical models, and to perform analyses with the numerical models and compare the results. The frequency domain software MIMOSA and the time domain software SIMO/RIFLEX coupled, with the SIMA graphical user interface, were used for the analyses. The numerical simulation was initially meant to be performed for two entirely different mooring systems, but due to problems, only a catenary mooring system has been analysed. The analyses show that the tension in the mooring lines and the offset of the moored vessel are comparable for both methods. The frequency domain yields the most conservative results, which is expected due to linearisations and simplifications made.

For the ALS analysis, the behaviour of a damaged mooring system was analysed. This was performed in time domain only, with a catenary mooring system, where one mooring line was broken. The analysis investigated the increased load on the remaining mooring lines, and also the effect of when the mooring line failed. The analysis show that for the remaining mooring lines in the cluster with a broken line, the mean tension increases by 21% and the max tension increases by 25%. Further analyses showed that the broken system was still robust against failure, with only a 0.03% chance of further failure, when entering a 100-year storm with one line broken and 100% minimum breaking strength (MBS). With a MBS degraded to 80%, the chance of failure was only 1.38%. The transient motion phase after a line failure was not necessarily the governing design criterion. For the specific condition analysed, the tension in the mooring lines was lower

when a mooring line failed during the storm, than it was when the failure took place before the storm. This means that the ultimate limit state design criterion was governing for this condition.

Sammendrag

I løpet av de siste årene har olje- og gassindustrien utvidet grensene for utvinning av olje og gass. Forankringssystemene har blitt mer komplekse, og antall brudd har vært uakseptabelt høyt. Det har vært hele 43 brudd på norsk sokkel i tidsrommet 2000 til 2013. Det er derfor interessant å sammenligne designverktøyet som industrien bruker til forankringsanalyser, og å undersøke oppførselen til et skadet forankringssystem.

Fokus i denne masteroppgaven har vært delt mellom en sammenlingning av forankringsanalyse i tids- og frekvensplan, og en undersøkelse av progressiv kollaps av et forankringssystem. Målet ved sammenligningen var å forstå teorien bak metodene, å verifisere, endre og forenkle modeller av forankringssystemet, og kjøre analyser med modellene og sammenligne resultatene. Frekvensplanprogrammet MIMOSA og tidsplanprogrammene SIMO, RIFLEX, med SIMA som grafisk brukergrensesnitt, ble brukt til analysene. Forankringsanalysene skulle egentlig bli utført for to vidt forskjellige forankringssystemer, men på grunn av problemer med den ene modellen i tidsplan, har analysene kun blitt utført for et slakt forankringsystem, med kjetting- og stålvaiersegmenter. Analysene viser at både strekket i forankringslinene og forskyvingen av platformen er sammenlignbare for begge metoder, til tross for helt forskjellig fremgangsmåte for å regne ut forskyving av flyteren og strekk i ankerlinene. Resultatene fra frekvensplanprogrammet MIMOSA gir de mest konservative resultatene, noe som er forventet ut i fra hvordan metoden er bygd opp.

For analysen av progressiv kollaps, ble oppførselen til et skadet forankringssystem analysert. Dette ble kun utført i tidsplan, med et slakt forankringssystem, hvor én ankerline ble brutt. Analysen undersøkte den økte belastningen på de gjenværende ankerlinene. Den undersøkte også effekter av *når* linen ble brutt. Analysen viste at i de gjenværende ankerlinene i samme hjørne, økte middelspenningen med 21% og maksimumspenningen økte med 25%. Videre analyser viste at det skadete forankringssystemet fremdeles var robust mot progressiv kollaps. Det var kun 0.03% sjanse for kollaps, når systemet ble simulert i en 100-års storm, med 100% av minimum bruddstyrke i de resterende ankerlinene. Hvis minimum bruddstyrke i ankerlinene ble redusert til 80%, var det kun 1.38% sjanse for kollaps. Analysen av tidspunkt for brudd, viste at den transiente fasen ikke

nødvendigvis var den mest kritiske. For den aktuelle analysen, ble strekket i ankerlinene mindre om bruddet skjedde mens miljøkreftene skapte den største forskyvingen, enn om bruddet skjedde før stormen. Dette betyr at ekstremrespons av et intakt system ble det gjeldende designkriteriet for denne tilstanden.

Preface

The work for this master's thesis concludes the degree of Master of Science in marine technology at the Norwegian University of Science and Technology. The thesis is weighted 30 ECTS and conducted during the spring of 2015.

I would like to thank my supervisor, Professor II Kjell Larsen, for taking great interest in teaching the theoretical background, to schedule weekly meetings, and always be available when needed. STATOIL is acknowledged through Kjell Larsen for providing input files for the semi submersible Snorre B and its mooring system.

I would also like to thank Vegard Øgård Aksnes at MARINTEK for helping out with the SIMA software, and troubleshoot problems with the taut-leg mooring system. A great thanks goes to Pål Levold, also at MARINTEK, for troubleshooting with the taut-leg mooring system. Unfortunately we were not able to solve the problems, and the focus of the thesis was slightly shifted.

Lastly, I would like to thank my fellow students at *Champagnesvingen*, for providing valuable discussion and insights.

Contents

List of Figures

List of Tables

Abbreviations

ALS	**A**ccidental **L**imit **S**tate
DAF	**D**ynamic **A**mplification **F**actor
DOF	**D**egree **O**f **F**reedom
FD	**F**requency **D**omain
FLS	**F**atigue **L**imit **S**tate
LF	**L**ow **F**requency
MBS	**M**inimum **B**reaking **S**trength
MPM	**M**ost **P**robable **M**aximum
NCS	**N**orwegian **C**ontinental **S**helf
NPD	**N**orwegian **P**etroleum **D**irectorate
PDF	**P**robability **D**ensity **F**unction
RAO	**R**esponse **A**mplitude **O**perator
SD	**S**tandard **D**eviation
sf	**s**afety **f**actor
TD	**T**ime **D**omain
ULS	**U**ltimate **L**imit **S**tate
WF	**W**ave **F**requency

Chapter 1

Introduction

Background

The purpose of a mooring system is to keep a floating vessel at a required position. This is done by connecting mooring lines, consisting of chain, wires or polyester rope, from the vessel to seabed anchors.

During the last years, the requirements to mooring systems have become more complex. The oil and gas industry is moving into new frontiers, i.e. ultra deep water and Arctic areas. As oil recovery of oil fields is increasing, the need for adjacent flotels and tender support vessels increases.

Mooring failure rate is unacceptably high, with 43 incidents between 2000 and 2013, only for the Norwegian Continental Shelf, (Brindley and Brandsæter, 2015). Some incidents have been multiline failure, leading to vessel drifting. The investigations show a variety of direct causes covering both inaccurate design, bad quality on mooring line components and lack of personnel competence related to operation of the system.

Because of the high failure rate, it is of interest to compare the analysis methods which are used by the industry today. A broken mooring line can take as long as six months to replace, (Larsen, 2015). A vessel with a broken line is therefore likely to experience rough conditions while its mooring system is damaged. It is thus interesting to investigate how a damaged mooring system will behave in a typical 100-year condition.

Scope of Work

The thesis is split into two parts, where the first part compares time and frequency domain analyses for the mooring system of a semi submersible. The latter part explores the behaviour after a line failure with a shallow water catenary mooring system.

The differences of the analysis methods are explored. Numerical simulations are performed, with the frequency domain software MIMOSA and the time domain software SIMO/RIFLEX coupled. The results are compared and discussed.

The thesis also explores a progressive collapse of the mooring system in a typical 100-year storm, with the added effect of the transient motion after a mooring line breaks. This is performed in the time domain with SIMO/RIFLEX coupled software.

Chapter 2

Theoretical Background

The mooring system for an offshore floater is designed against overload of the tension for the mooring lines. The tension of a mooring line is governed by the top end motion of the mooring line, i.e. the static offset and the dynamic motion.

In other words, the design of a mooring system starts with calculating the top end motion. To do this, the equation of motion, equation 2.5, presented in chapter 2.2, must be solved for all six degrees of freedom. Once the motion is calculated, the tension in the mooring lines can be found. How these calculations are performed, is presented next.

2.1 Rigid Body Motions

Before further theory can be presented, the rigid body motions have to be defined. The motions of floating structures can be divided into static and dynamic motion, where the static motion is the mean offset, and the dynamic motion is wave-frequency motion, high-frequency motion and low frequency motion. The high frequency motion is not important for a moored semi submersible. The oscillatory rigid body translatory motions are referred to as surge, sway and heave, and are denoted η_1, η_2 and η_3, respectively. The oscillatory angular motions are referred to as roll, pitch and yaw and are denoted η_4, η_5 and η_6,respectively. All six rigid body motions can be seen in figure 2.1.

The motion of an arbitrary position on the vessel, e.g. the fairlead, is expressed in equation 2.1

$$s = \eta_1 i + \eta_2 j + \eta_3 k + \omega \times r \tag{2.1}$$

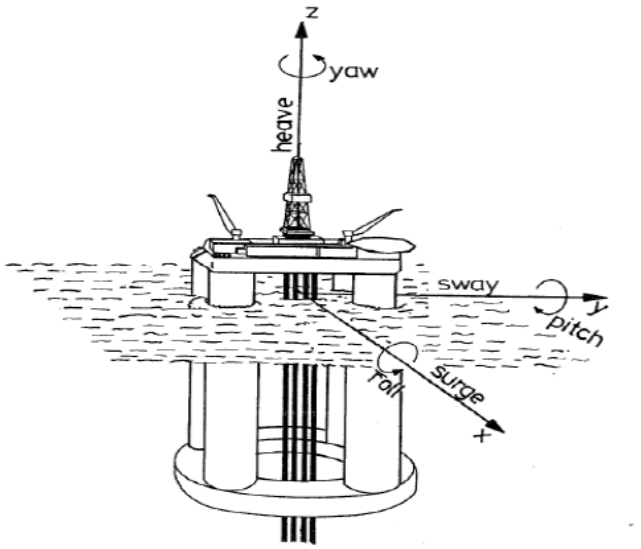

FIGURE 2.1: Rigid-body motions,(Faltinsen, 1990)

where ω and r are defined in equations 2.2 and 2.3, respectively.

$$\omega = \eta_4 i + \eta_5 j + \eta_6 k \tag{2.2}$$

$$r = xi + yj + zk \tag{2.3}$$

When expanding equation 2.1, the contributions to the total translatory motions are found, see equation 2.4.

$$s = \eta_1 i + \eta_2 j + \eta_3 k + \begin{vmatrix} i & j & k \\ \eta_4 & \eta_5 & \eta_6 \\ x & y & z \end{vmatrix} = (\eta_1 + z\eta_5 - y\eta_6)i + (\eta_2 + x\eta_6 - z\eta_4)j + (\eta_3 + y\eta_4 - x\eta_5)k \tag{2.4}$$

The translatory motion for an arbitrary position is dependent on the translatory motion of the floater in the given direction, in addition to the product of the angular motions of the floater and the coordinates of the arbitrary position.

2.2 Equation of Motion

Equation 2.5 must be solved for all six degrees of freedom to find the top end motion.

$$(M + A(\omega))\ddot{x} + \int_0^t h(t-\tau)\dot{x}(\tau)d\tau + D_l\dot{x} + D_q\dot{x} \mid \dot{x} \mid + K(x)x = Q(t, x, \dot{x}) \tag{2.5}$$

Where M is the mass matrix, $A(\omega)$ is the frequency dependent added mass matrix, x is the position vector, $h(\tau)$ is the retardation function, D_l is the linear damping matrix, D_q is the quadratic damping matrix, K(x) is the non-linear stiffness matrix and $Q(t, x, \dot{x})$ is the excitation force vector, defined in equation 2.6. The terms will be explained in detail in the following chapters.

$$Q(t, x, \dot{x}) = q_{waves} + q_{wind} + q_{current} \tag{2.6}$$

The environmental loads, shown in equation 2.6, have different frequencies, and can be divided into excitation regimes, seen in table 2.1

The excitation frequencies are compared to the natural oscillation frequencies for a semi submersible, for all six DOFs, seen in table 2.2, and a frequency ratio is established. The in-plane DOFs, surge, sway and yaw, will have motion contributions from static forces, WF forces and LF forces, while the out-of-plane DOFs, heave, roll and pitch, will only be affected by the WF-forces.

Excitation	**Static**	**Wave-frequency**	**Low-frequency**
Waves	Mean 2nd order	1st order forces	Low frequency 2nd order forces
Wind	Mean wind speed		Wind gust
Current	Mean current speed		

Table 2.1: Excitation regimes

In table 2.1, the high frequency is of minor importance and is therefore omitted.

Surge	Sway	Heave	Roll	Pitch	Yaw
$\geq$ 100 s	$\geq$ 100 s	20-25 s	45-60 s	45-60 s	$\geq$ 100 s

Table 2.2: Natural oscillation periods for a semi submersible

$$Frequency \quad ratio = \frac{Excitation frequency}{Natural frequency} = \frac{\omega}{\omega_0} \tag{2.7}$$

The frequency ratio governs the value of the dynamic amplification factor, seen in equation 2.8. The dynamic amplification factor is the relation between dynamic and static response for a given load.

$$DAF = \frac{1}{\sqrt{(1 - (\frac{\omega}{\omega_0})^2)^2 + \omega^2 \frac{c^2}{k^2}}} \tag{2.8}$$

The plot of the dynamic amplification factor, as a function of frequency ratio, can be seen in figure 2.2.

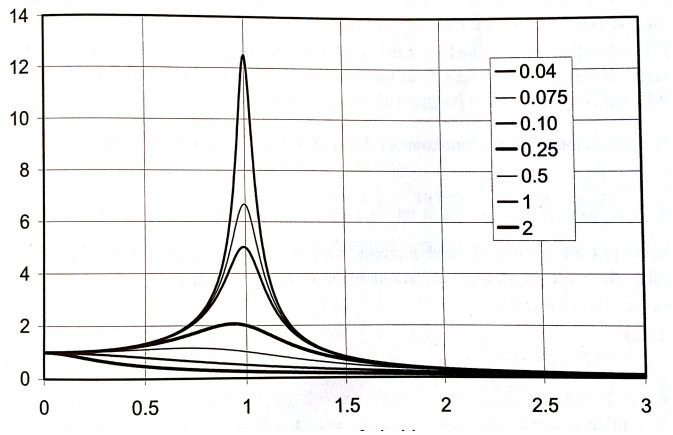

FIGURE 2.2: Dynamic amplification factor as a function of frequency ratio, for different values of the damping ratio,(Larsen, 2012)

The plot is split into three domains, based on which forces are the dominating balancing forces. These domains are

- Resonance dominated
- Inertia dominated
- Stiffness dominated

The domains will be explained in chapter 2.2.2, 2.2.3 and 2.2.4

2.2.1 Excitation

First Order Wave Forces

Moored vessels are exposed to large first order wave forces, which are the only contribution to the wave frequency motion for mooring analysis. These are linearised motions, and they are proportional to the wave height. The time averaged value of the first order wave motion is zero. The first order forces are typically calculated by potential theory programs like WAMIT.

Second Order Wave Forces

Moored vessels are also exposed to smaller, second order mean and low frequency wave forces and moments proportional to the square of the wave height. Low frequency wave forces are normally an order of magnitude smaller than wave frequency forces. Even so, their effect may be significant since the low frequencies are close to natural frequencies of the system, (Løken and Hagen, 1999). The second order wave forces result in mean forces, and forces oscillating with difference frequency or sum frequencies in addition to the linear solution. Mean and slowly-varying wave loads (difference frequency loads) are of importance in the design of mooring systems, (Faltinsen, 1990). Sum frequency loads can excite oscillations if the structure's natural period is low (2-3 seconds), but this is not relevant for a moored semi submersible.

Wind Forces

Wind forces will contribute with a mean force and a slowly varying gust force. The mean wind force will lead to a mean offset. Faltinsen (1990) has also described that the wind gust can produce slowly-varying oscillations of marine structures for surge, sway and yaw. This is caused by wind gusts with significant energy at the same order of magnitude as the natural frequencies for surge, sway and yaw, see table 2.2.

The time dependent wind velocity is described in equation 2.9, where $\bar{U}$ is the mean wind velocity and $u(t)$ is the dynamic wind gust, with a zero mean.

$$U(t) = \bar{U} + u(t) \tag{2.9}$$

The force from the wind is described in equation 2.10.

$$q_{wind}(t) = \frac{1}{2} \cdot \rho_{air} \cdot C_D \cdot A \cdot (U(t) - \dot{x}_{LF})^2 \tag{2.10}$$

Where ρ_{air} is the density of air, C_D is the global drag coefficient of the floater , A is wind area of the floater, and $\dot{x}_{LF}$ is the velocity of the floater.

The force is proportional to the square of the relative velocity between the wind and the floater.

In equation 2.10, the constant terms are established as a coefficient, seen in equation 2.11.

$$c_{wind} = \frac{1}{2} \cdot \rho_{air} \cdot C_D \cdot A \tag{2.11}$$

Equation 2.9 and 2.10 are then combined, and the wind coefficent is introduced. When neglecting terms of minor importance, the result is

$$q_{wind}(t) \approx c_{wind} \cdot \bar{U}^2 + c_{wind} \cdot 2 \cdot \bar{U} \cdot u(t) - c_{wind} \cdot 2 \cdot \bar{U} \cdot \dot{x}_{LF} \tag{2.12}$$

In equation 2.12, the first term represents the static wind force, the second term represents the LF excitation force, and the third term represents the LF damping force.

Current Forces

There exists no gust model for current velocity, so it is assumed to be constant with respect to time. The force from the current is described in equation 2.13.

$$q_{current}(t) = \frac{1}{2} \cdot \rho_{water} \cdot C_D \cdot A \cdot |\bar{V} - \dot{x}_{LF}|(\bar{V} - \dot{x}_{LF}) \tag{2.13}$$

where ρ_{water} is the density of water, C_D is the global drag coefficient of the floater, A is the current area, $\bar{V}$ is the current velocity and $\dot{x}_{LF}$ is the floater velocity.

The force is proportional to the square of the relative velocity between the current and the floater.

In equation 2.13, the constant terms are established as a coefficient, seen in equation 2.14.

$$c_{current} = \frac{1}{2} \cdot \rho_{water} \cdot C_D \cdot A \tag{2.14}$$

Equation 2.13 is then expanded and the current coefficient is introduced. When neglecting the term of minor importance, the result is equation 2.15.

$$q_{current}(t) \approx c_{current} \cdot \bar{V}^2 - c_{current} \cdot 2 \cdot \bar{V} \cdot \dot{x}_{LF} \tag{2.15}$$

In equation 2.15 the first term represents the static current force, and the second term represents the LF damping force.

2.2.2 Low Frequency Damping

Damping forces drain energy from the system, and thus limits the response. This is especially important when the frequency ratio is close to 1, as shown in figure 2.3. In this resonance dominated domain, the excitation cannot be balanced by either inertia or stiffness forces. With no or too little damping, the system will be excited in resonant motion until collapse.

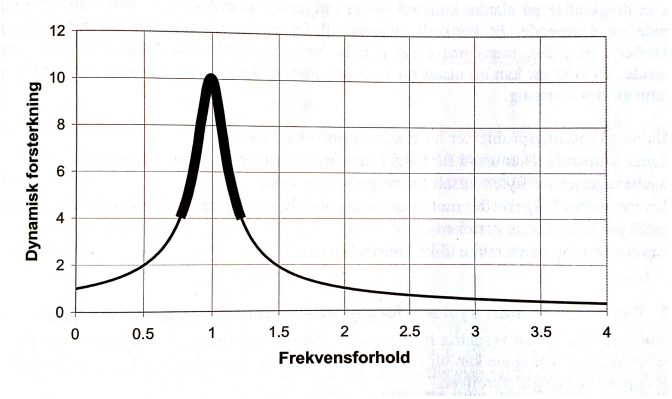

FIGURE 2.3: Resonance dominated domain,(Larsen, 2012)

Table 2.2 shows the natural oscillation periods for all six DOFs. The in-plane DOFs, i.e. surge, sway and yaw, are low frequent, and in the same frequency magnitude as the wind gust and 2nd order wave forces. The damping forces must therefore balance these terms. The most important damping contributions for a semi submersible are the following

- Viscous loads of floater hull
- Wave drift damping
- Drag forces on mooring lines
- Damping due to wind and current

The contributions will be explained in detail next.

Viscous Loads on Floater Hull

The viscous loads on the floater hull can be divided into skin friction effects and viscous effects due to the pressure distribution around the vessel. The latter effect is associated with eddy making and is therefore called eddy-making damping. The eddy-making damping can be quite large for rectangular cross sections, (Faltinsen, 1990). For a semi-submersible, viscous force on the columns and pontoons is the main source of damping, (Lie and Moan, 2007).

Wave Drift Damping

Wave drift damping is due to change in the mean drift force on a body when it moves with constant speed in the direction of the waves. It is proportional to the square of the incoming wave amplitude and proportional to the slowly- varying velocity of the body.

Wave drift damping is caused by waves and can be seen by comparing free-decay model tests of a ship in still water and in regular waves, see figure 2.4. The wave-drift damping in surge can be explained by interpreting the slow-drift surge motion as a quasi-steady forward and backward speed. It is well known that the added resistance of a ship in waves is speed dependent, (Faltinsen, 1990)

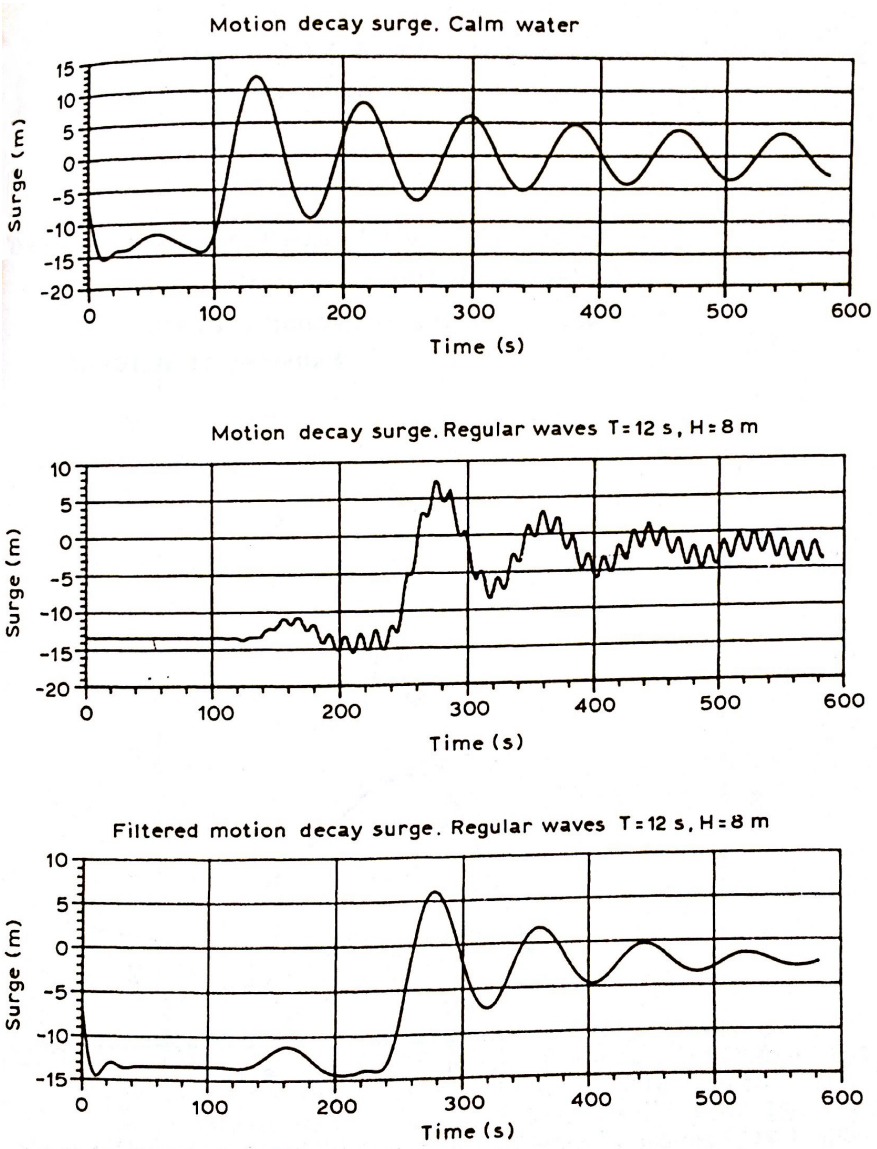

FIGURE 2.4: Influence of wave-drift damping in surge,(Faltinsen, 1990)

It is observed that the motion decays faster with waves present.

Wind and Current

The wind and current damping contributions are due to the drag forces from the relative motion between the wind and current, and the floater, as seen in chapter 2.2.1.

Drag Forces on Mooring Lines

The top end motion will introduce dynamic lateral movement on the mooring lines. This lateral movement will in turn introduce drag forces. The drag forces will drain energy from the system, i.e. create a damping force. The mooring line damping can contribute 30%-40% of the total damping for a semi submersible, (Lie and Moan, 2007). A simplified dynamic model for estimating the mooring line damping can be found in (Lie and Moan, 2007).

This damping contribution is increased with water depth, as the horizontal top end motion is larger and the suspended length is also larger, (Næss and Moan, 2013).

2.2.3 Inertia

The inertia forces are proportional to the acceleration, and consists of physical mass and added mass.

When the load frequency is higher than the natural frequency, the system's inertia forces balance the excitation forces, i.e. the system is inertia dominated. The environmental forces are perceived as too rapid, and the large inertia of the system ensures that the system doesn't react quickly enough. This is the case for first order wave forces in surge, sway and yaw.

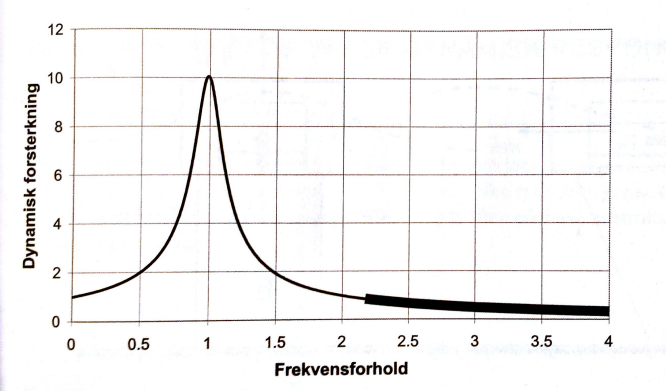

FIGURE 2.5: Inertia dominated domain,(Larsen, 2012)

2.2.4 Stiffness

The stiffness is created by the mooring system. There are two contributions to the total stiffness of one mooring line. The two contributions are geometric stiffness and elastic stiffness, and they act like two springs in series. The resulting stiffness is found in equation 2.16

$$\frac{1}{k_{total}} = \frac{1}{k_{geometric}} + \frac{1}{k_{elastic}} \tag{2.16}$$

Geometric Stiffness

Geometric stiffness results from the equilibrium of moments for a catenary mooring line. In equilibrium position, a large segment of the mooring line will lie on the seabed. When moved away from its equilibrium position, the suspended length of the mooring line will increase. This has two effects, i.e. the total force will increase, and the moment arm will also increase. Both these effects will cause a restoring force back to equilibrium position. The concept can be seen in figure 2.6.

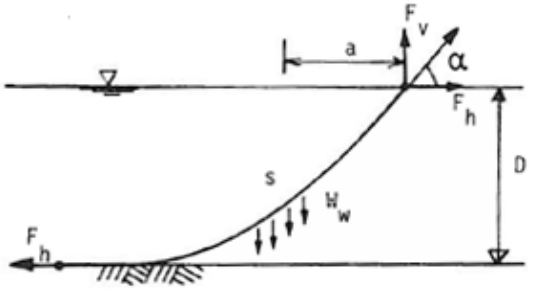

FIGURE 2.6: Catenary mooring line,(Larsen, 2014a)

In equation 2.17 F_h is the restoring force, D is the water depth, a is the moment arm and W_w is the weight of the mooring line in water. When the offset is increased, both the moment arm and the weight of the mooring line are increased, which results in a *non-linear correlation between the restoring force and the offset*

$$F_h = \frac{W_w \cdot a}{D} \tag{2.17}$$

Figure 2.7 shows the forces on an element of a mooring line. Forces D and F acting on the element are the mean hydrodynamic forces per unit length in the normal and tangential direction, respectively. w is the weight per unit length of the line in water, A is the cross-sectional area of the mooring line, E is the elastic modulus and T is the line tension, (Faltinsen, 1990)

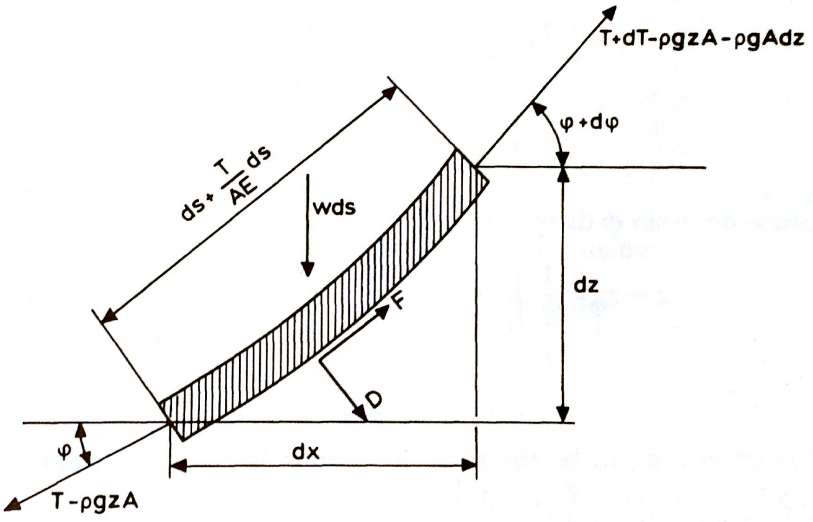

FIGURE 2.7: Forces on a mooring line element, (Faltinsen, 1990)

From figure 2.7, the catenary equations, 2.18 and 2.19, can be found. These equations are non-linear and it is in general not possible to find an explicit solution. Further information on the catenary equation can be found in (Faltinsen, 1990)

$$dT - \rho g A dz = [w sin\phi - F(1 + \frac{T}{AE})]ds \tag{2.18}$$

$$Td\phi - \rho g A z d\phi = [w cos\phi + D(1 + \frac{T}{AE})]ds \tag{2.19}$$

It is of interest to find the line characteristics of a mooring line, i.e. the relation between the horizontal offset and the tension of the line. This can be done by manipulating equations 2.18 and 2.19, assuming the line is inelastic, i.e when $\frac{T}{EA} \ll 1$, and use figure 2.8. For the complete derivation, see (Larsen, 2014b). The relation is seen in equation 2.20, where X_l is the horizontal distance to the anchor, T_x is the horizontal tension, w is the weight in water and y is the water depth.

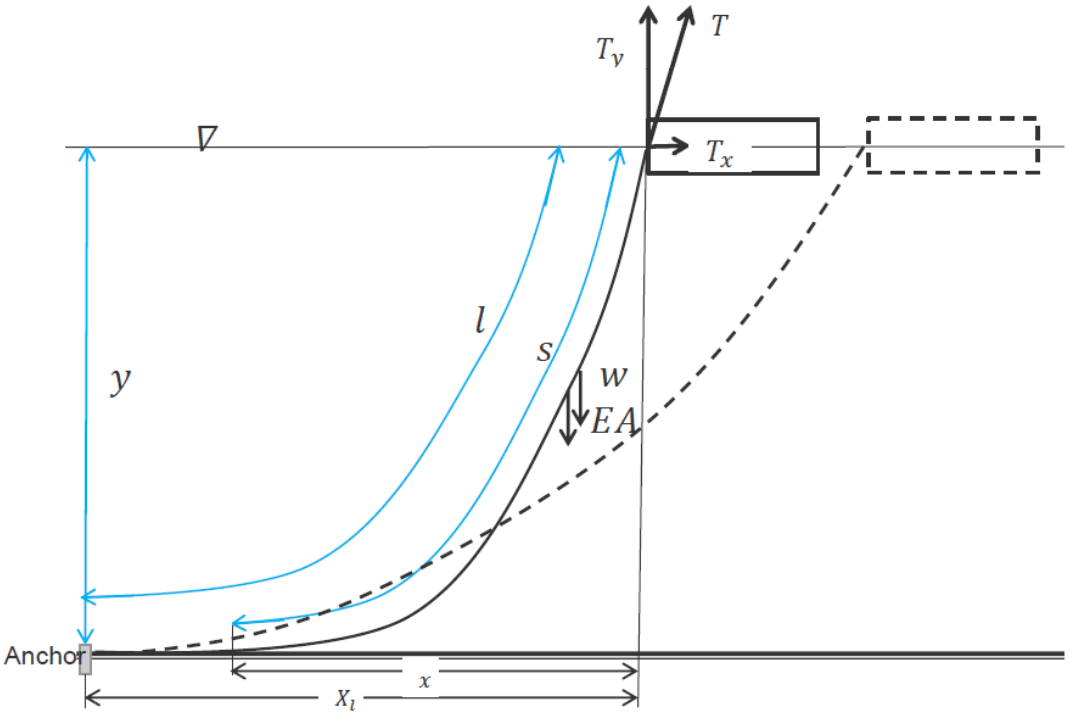

FIGURE 2.8: Illustration of the notation defining the line characteristics, (Larsen, 2014a)

$$X_l = l + \frac{T_x}{w} \cdot cosh^{-1}(1 + \frac{w \cdot y}{T_x}) - \sqrt{y \cdot (y + \frac{2T_x}{w})} \tag{2.20}$$

Since the weight of the catenary mooring system is getting very large for increasing water depths, the concept is not applicable for large water depths.

Elastic Stiffness

Elastic stiffness results from the elastic elongation of the mooring line. The mooring line will act like a mechanical spring, and when pulled out of its equilibrium position, it will create a restoring force back to equilibrium position. This effect is most important for a taut-leg system, where there is a polyester fibre spanning almost the whole height of the water column.

The concept can be seen in figure 2.9.

In equation 2.21, k is a spring constant, i.e. *the restoring force F_h is linearly correlated with the offset x*, when disregarding the change in angle, $\Delta\alpha$.

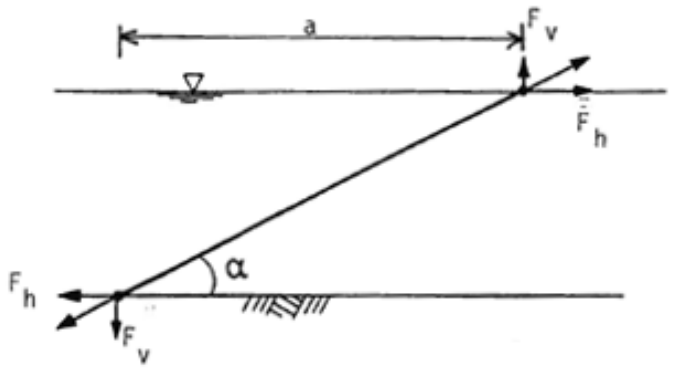

FIGURE 2.9: Taut-leg mooring line, (Larsen, 2014a)

$$F_h = F \cdot \cos\alpha = k \cdot x \cdot \cos\alpha \tag{2.21}$$

Restoring Force

When equation 2.20 is established for all mooring lines, the total restoring force can be found by combining the contribution for each line. This is shown in equations 2.22, 2.23 and 2.24 and figure 2.10.

$$F_{Restoring,Surge} = \sum_{i=1}^{n} T_{xi} cos\psi_i \tag{2.22}$$

$$F_{Restoring,Sway} = \sum_{i=1}^{n} T_{xi} sin\psi_i \tag{2.23}$$

$$F_{Restoring,Yaw} = \sum_{i=1}^{n} T_{xi}[x_i sin\psi_i - y_i cos\psi_i] \tag{2.24}$$

Figures 2.11 and 2.12 show examples of the restoring force as a function of offset, which is the total horizontal force exerted by all the mooring lines due to a horizontal offset from equilibrium position. The position dependent stiffness can be seen as the derivative of the restoring force at the position of interest.

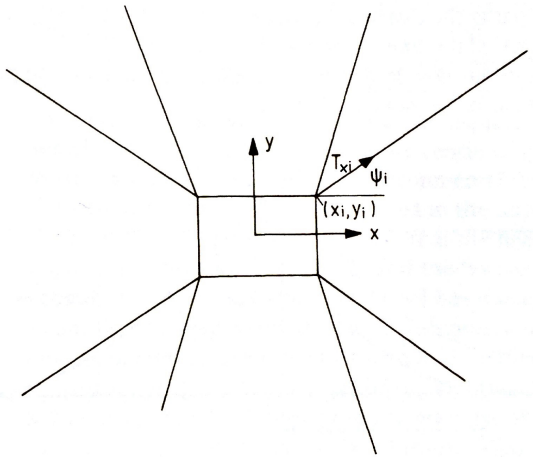

FIGURE 2.10: Notation for computing total horizontal restoring force, (Faltinsen, 1990)

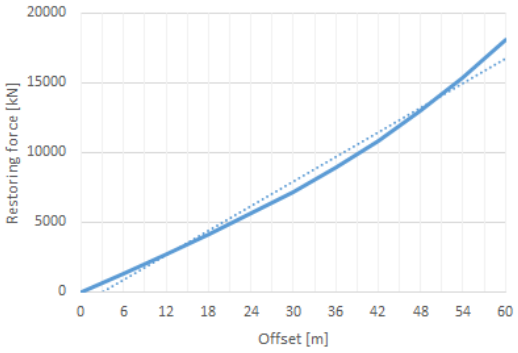

FIGURE 2.11: Catenary system: non-linear restoring force

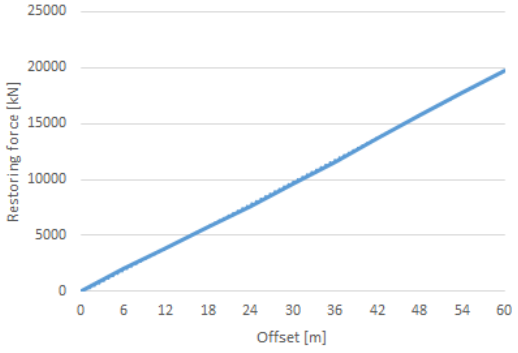

FIGURE 2.12: Taut-leg system: linear restoring force

2.3 Time and Frequency Domain

A stochastic process can be analysed in either frequency or time domain. The two methods pose different advantages and drawbacks. In the next chapters, the methods will be explained in detail, and the advantages and drawbacks will be elaborated.

The methods differ on how the equation of motion is solved, and also how the line tension is calculated based on the motion.

2.3.1 Time Domain

In the time domain, the stochastic process is described through a realization of the response. Realizations for different time periods give different *time series of the process*. The main response parameters obtained from the time series are processed statistically

to yield extreme values. The time domain simulation should be long enough to yield stable statistical values, (ISO Standard, 2013).

Furthermore, the equation of motion is solved by direct numerical integration, which greatly increases computational time, but also offers a lot of advantages. The integration is performed for each time step, which does not exclude non-linear effects. The boundary conditions can also be changed during the simulation.

The added mass and damping are generally frequency dependent. In time domain they can be Fourier transformed to give the so called retardation functions, denoted $h(\tau)$,(Low and Langley, 2007). The retardation functions are, due to numerics, preferably calculated based on damping, (Larsen, 2014a). In equation 2.5, the retardation functions, 2.26, are introduced into the equation of motion for a single DOF.

$$(M + A_\infty)\ddot{x} + \int_0^t h(t-\tau)\dot{x}(\tau)d\tau + D_l\dot{x} + D_q\dot{x} \mid \dot{x} \mid + K(x)x = Q(t, x, \dot{x}) \tag{2.25}$$

$$h(\tau) = \frac{2}{\pi}\int_0^\infty C(\omega)cos(\omega\tau)d\omega = -\frac{2}{\pi}\int_0^\infty \omega A(\omega)cos(\omega\tau)d\omega \tag{2.26}$$

To compare the results from time domain with the results from frequency domain, statistical tools have to be employed on the generated time series from the time domain. A Gumbel distribution can be used to find the most probable max mooring line tension and offset. The error of the estimate is reduced with increasing simulation length and number of simulations the distribution is based on.

To compare the low frequency or wave frequency values from time domain with values from frequency domain, the signal from the time series must be filtered.

From Top End Motion to Mooring Line Tension

To find the mooring line tension from a time domain analyses, analyses have to be performed with a seed number variation. Typically, at least 10-20 simulations should be performed for a 3 hour sea state, (Larsen, 2015). This is because time domain simulations give statistical uncertainties, and the simulations should be both of a certain length and a certain number of simulations. The parameter of interest, e.g. maximum mooring

line tension, can then be extracted from each analysis, and a statistical model can then estimate the true value.

Furthermore, there are two different methods applied, i.e a coupled and decoupled model.

The decoupled model uses two different models for the mooring system and the vessel. The vessel motion is simulated first, and then the mooring tensions are simulated by the mooring system model, with the vessel motion as input.

The coupled model uses a complete model of mooring system and vessel, and simulate the tension and motion simultaneously. This is done by simulating the motion and forces for each time step, and use the results as input for the next time step. Both the coupled and decoupled approach can be seen in figure 2.13

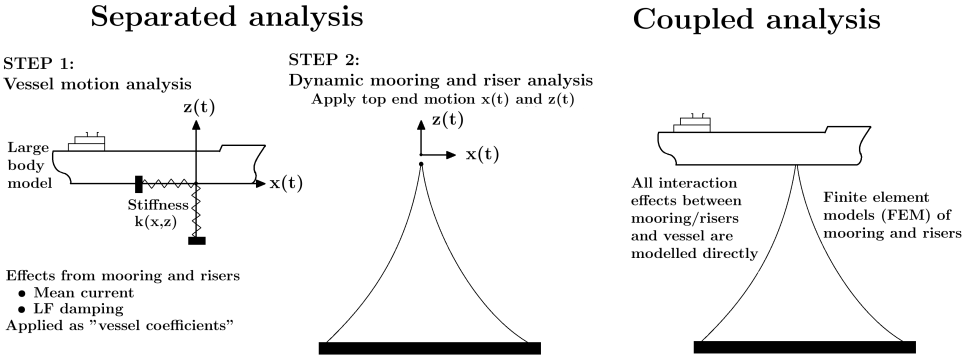

FIGURE 2.13: Coupled and decoupled approach,(Ormberg and Larsen, 2004)

2.3.2 Frequency Domain

In the frequency domain, a stochastic process is described through an *energy spectrum*. An energy spectrum is a way of representing the energy of a stochastic process as a function of frequency. It gives a complete description of the Gaussian process' statistical properties, such as standard deviation, zero up-crossing period and extreme values. Given that the spectral moments can be calculated accurately, all the statistical parameters can be computed without any statistical uncertainty,(Larsen, 2012). The calculations are based on the principle of linear superposition, i.e. the total response is the sum of responses for each frequency component.

The most developed and widely used frequency domain solution techniques require linear equations of motion. The linear assumption is also predominant in the random process

theory used to interpret the solution. This is inconvenient when modelling drag loads, time varying geometry, horizontal restoring forces and variable water surface elevation, since these effects are non-linear. In some cases, these non-linearities can be satisfactorily linearised, (Løken and Hagen, 1999)

The frequency domain requires far less computational power than a full time domain analysis. It is also possible to include frequency dependent added mass and damping, without use of retardation functions. A frequency domain analysis is better suited for moderate sea states than severe sea states, when the non-linearities become too significant.

As mentioned, the equation of motion, equation 2.5, is not solved by use of retardation functions, but split into contributions from low frequency and wave frequency, see equation 2.27 and 2.28.

$$x = x_{LF} + x_{WF} \tag{2.27}$$

$$Q = Q_{LF} + Q_{WF} \tag{2.28}$$

Furthermore, the motions are required to be linear responses to waves, which means that the damping and stiffness must be linearized, (Løken and Hagen, 1999).

Low frequency

The resulting *low frequency* equation of motion can be seen in equation 2.29.

$$(M + A(0)) \cdot \ddot{x}_{LF} + D_{lin} \cdot \dot{x}_{LF} + K_{lin} \cdot x_{LF} = q_{wavedrift} + q_{wind} \tag{2.29}$$

Added mass is frequency dependent, hence the A(0) is for low frequency

Then the frequency response method is used to create a relation between the spectrum for the low frequency load and the spectrum for the low frequency motion.

$$S_{xLF}(\omega) = \mid H(\omega) \mid^2 \cdot S_{qLF}(\omega) \tag{2.30}$$

where $S_{xLF}(\omega)$ is the low frequency spectrum for the motion, $S_{qLF}(\omega)$ is the low frequency spectrum for the load and $H(\omega)$ is the response amplitude operator.

The low frequency spectrum for the loads has two contributions, the second order wave spectrum and the wind spectrum

$$S_{qLF}(\omega) = S_{qwavedrift}(\omega) + S_{qwind}(\omega) \tag{2.31}$$

which can can be seen in equation 2.32 and 2.33, respectively.

$$S_{qwavedrift}(\mu) = 8 \cdot \int_0^\infty c_{wa}(\omega + \frac{\mu}{2}) \cdot c_{wa}(\omega + \frac{\mu}{2}) \cdot S_\eta(\omega) \cdot S_\eta(\omega + \mu) d\omega \tag{2.32}$$

where c_{wa} are the wave drift force coefficients and $S_\eta(\omega)$ is the wave spectrum.

$$S_{qwind}(\omega) = (\rho_{air} \cdot C_D \cdot A \cdot \bar{U})^2 \cdot S_{windvelocity}(\omega) \tag{2.33}$$

Where ρ_{air} is the density of air,C_D is the global drag coefficient, A is the wind area, $\bar{U}$ is the mean wind velocity and $S_{windvelocity}(\omega)$ is the wind velocity spectrum.

The response amplitude operator can be expressed as

$$\mid H(\omega) \mid^2 = \frac{1}{(K *_{lin} -[M + A(0) \cdot \omega^2]^2 + D *_{lin}^2 \cdot \omega^2)} \tag{2.34}$$

Wave frequency

For the wave frequency, the equation of motion becomes

$$(M + A(\omega)) \cdot \ddot{x}_{WF} + C(\omega) \cdot \dot{x}_{WF} + D_l \cdot \dot{x}_{WF} + K \cdot x_{WF} = Q_{WF}(t, x, \dot{x}) \tag{2.35}$$

The response amplitude operator can be established in a similar way, see equation 2.36

$$H_{WF}(\omega) = \frac{x_{WF,a}(\omega)}{\eta_a(\omega)} \tag{2.36}$$

where $\eta_a(\omega)$ is the wave elevation amplitude and $x_{WF,a}(\omega)$ is the WF motion amplitude.

When the maximum and significant offset for both wave frequency and low frequency are found, they are combined according to the "combination rule", stated in equation 2.37. See also figure 2.14

$$X_{max,total} = max \begin{cases} \bar{X} + X_{LF,max} + X_{WF,sign} \\ \bar{X} + X_{WF,max} + X_{LF,sign} \end{cases} \tag{2.37}$$

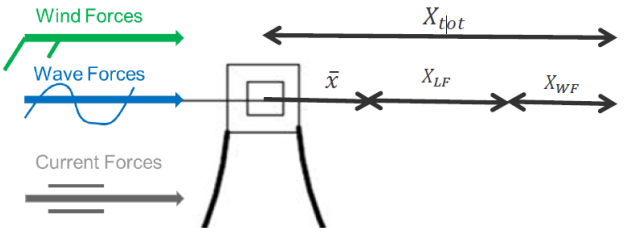

FIGURE 2.14: Combination rule,(Larsen, 2014a)

Where $\bar{X}$ is the static offset. When the total max offset has been found, the forces are calculated in either a quasi-static or dynamic analysis.

From Top End Motion to Mooring Line Tension

The mooring line tension can be calculated by either a quasi-static analysis or dynamic analysis. These methods will be presented next.

Quasi-Static Analysis

In this approach, the wave actions are taken into account by statically offsetting the structure by wave-induced motions. Dynamic actions on the mooring lines associated with mass, damping and fluid acceleration are neglected. The line characteristics, found in section 2.2.4, are used to find the mooring line tension. Research in mooring line dynamics has shown that the reliability of mooring designs based on this method can

vary widely depending on the structure type, water depth and line configuration, (DNV GL, 2013)

Dynamic Analysis

Dynamic analysis of the mooring lines accounts for the time-varying effects due to mass, damping and fluid acceleration. In this approach, the time-varying fairlead motions are calculated from the structure's surge, sway, heave, roll, pitch and yaw motions. Dynamic models are used to predict mooring line responses on the fairlead motions, (DNV GL, 2013).

The tension is found by adding the motion contributions from static, low frequency and wave frequency, seen in equation 2.37. The maximum wave frequency motion is then subtracted, to find the position X_{base}, with the corresponding tension T_{base}. Then the dynamic wave frequency motion is simulated around this point, see figure 2.15.

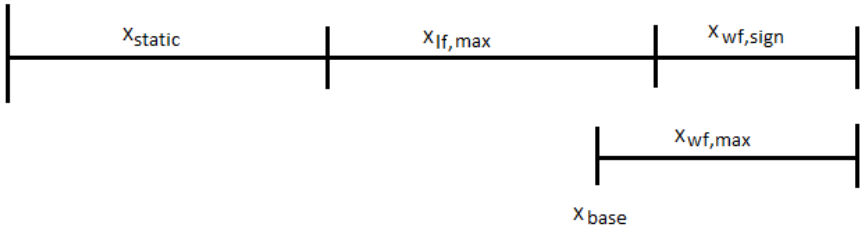

FIGURE 2.15: Illustration Dynamic Computation MIMOSA

The characteristic tension, which is the most probable max tension during a 3-hours in the worst 100-year sea state, can then be expressed in equation 2.38.

$$T_C = T_{base} + \sigma_T \sqrt{2lnN} \tag{2.38}$$

where σ_T is the standard deviation of the top end line tension. See equation 2.39.

$$\sigma_T = \sqrt{\int_0^\infty S_T(\omega) d\omega} \tag{2.39}$$

where S_T is the spectrum of the top end line tension.

2.4 Extreme Value Statistics

The time domain results are given as time series. To obtain characteristic values, extreme value statistics is utilised. The following theory is found in (Leira, 2010).

The instantaneous surface elevation is assumed to be Gaussian distributed and narrow-banded, so that all maxima are identically Rayleigh distributed. All maxima are also assumed to be statistically independent.

When these assumptions are satisfied, the Gumbel distribution can be used to find the characteristic value most probable max (MPM). This is roughly at the 37% quantile of the Gumbel distribution.

The Gumbel distribution is an extreme value distribution, where the samples are $y_1, y_2, ..., y_N$, and the y samples are $y = max(x_1, x_2, ..., x_N)$.

The Gumbel distribution is expressed in equation 2.40 and 2.41.

$$F_y(y) = e^{(-e^{-\alpha(y-u)})} \qquad -\infty < y < \infty \tag{2.40}$$

$$f_y(y) = \alpha e^{(-\alpha(y-u)e^{-\alpha(y-u)})} \tag{2.41}$$

where $F_y(y)$ is the cumulative density function, $f_y(y)$ is the probability density function and α and u are moment estimators. These can be seen in equation 2.42 and 2.43.

$$\hat{\alpha} = \frac{1}{\hat{s}_y}\frac{\pi}{\sqrt{6}} = \frac{1.28255}{\hat{s}_y} \tag{2.42}$$

$$\hat{u} = \hat{\mu}_y - \hat{s}_y\frac{\sqrt{6}}{\pi}0.57722 = \hat{\mu}_y - 0.45\hat{s}_y \tag{2.43}$$

$\hat{\mu}_y$ and $\hat{s}_y$ are the mean and standard deviation, respectively, and are found from the sample of extreme values.

Chapter 3

System description

The system analysed, including both the semi submersible and mooring system, will be presented here. The description covers characteristics of wind forces, current forces, and first order motion RAOs.

3.1 The Semi Submersible

The model analysed is based on the Snorre B semi submersible design. The platform is a combined drilling and production platform. A ring pontoon and four columns comprise the hull, and it is symmetric about both the y and x axes. The main particulars can be seen in table 3.1

Displacement	56600 [ton]
Operational Draught	21.0 [m]
Air gap	20 [m]
Width of columns	17.5 x 17.5 [m^2]
Center-to-center distance columns	67.5 [m]
Pontoon width	17.5 [m]
Pontoon height	8.5 [m]
GM	2.5 [m]

TABLE 3.1: Main particulars, (Statoil)

The current coefficients, wind coefficients, wave drift coefficients and motion RAOs are all given as input, and they are calculated based on the geometry of Snorre B. They are all plotted in appendix A, and the RAO for surge and heave can also be seen in figure 3.1 and 3.2, respectively.

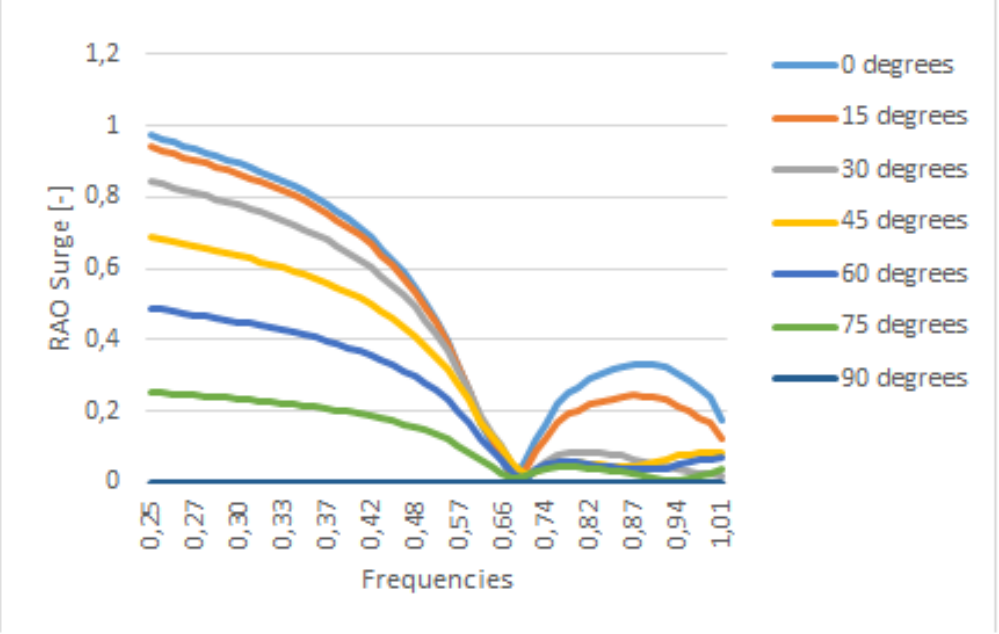

FIGURE 3.1: Surge motion RAO

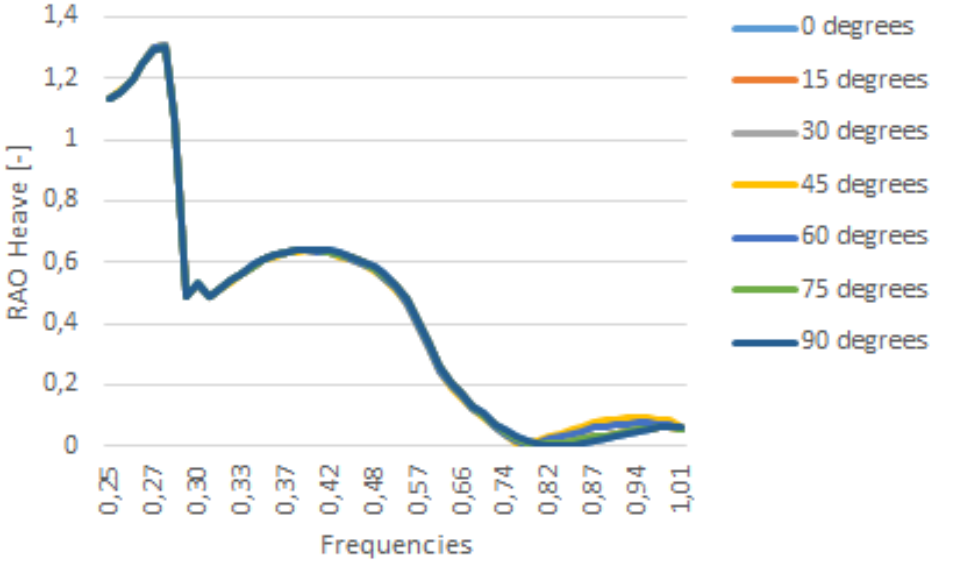

FIGURE 3.2: Heave motion RAO

Degree of freedom	Period [s]
Surge	130
Sway	120
Heave	22,2
Roll	53
Pitch	56
Yaw	72

TABLE 3.2: Natural oscillation periods, (Statoil)

Table 3.2 show the natural oscillation periods for Snorre B. Although the model has been modified, the natural oscillation periods are believed remain the same.

3.2 The Mooring System

The semi submersible platform model, described in chapter 3.1, has been analysed with two different mooring systems. The first system is a catenary type system in 350 meter water depth, which is the actual mooring system of Snorre B, with some simplifications. The second system is a taut-leg polyester type system in 1500 m water depth.

For both systems the lines are defined by specifying the fairlead coordinates, the horizontal angle and the pretension. The anchor coordinates and the length of each line are then computed. The fairlead coordinates, the horizontal angle and the pretension are set equal for both systems. It is the different properties of the mooring lines and water depth that accounts for the different mooring line lengths and anchor coordinates for the two systems. The input files for the mooring systems can be seen in appendix B. A definition of the mooring line number and the general layout for both systems can be seen in figure 3.3.

Catenary System

For the catenary system, each line consists of platform chain, steel wire and bottom chain. The sixteen mooring lines are grouped in four clusters. See figure 3.4

The specifics of the catenary system can be seen in table 3.3. In table 3.3 and 3.4, the segment numbering starts at the anchor.

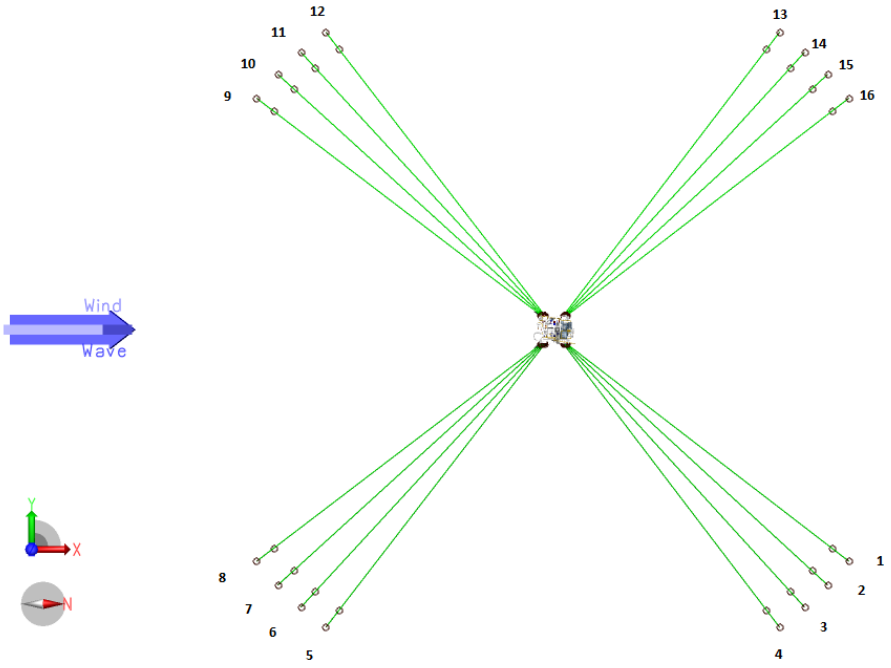

FIGURE 3.3: Horizontal projection of mooring lines for both systems

Segment	Segment type	Diameter	Length	E-modulus	Weight in water
1	Chain	137 [mm]	800 [m]	39000 [MPa]	3,244 [kN/m]
2	Steel wire	148 [mm]	285 [m]	90700 [MPa]	0,688 [kN/m]
3	Chain	137 [mm]	25 [m]	39000 [MPa]	3,244 [kN/m]
4	Chain	145 [mm]	92,9 [m]	36900 [MPa]	3,852 [kN/m]

TABLE 3.3: Catenary system

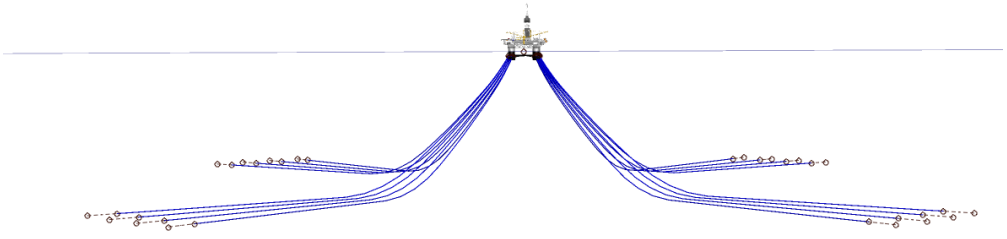

FIGURE 3.4: Catenary mooring system

Taut-leg System

For the taut-leg system, the number of mooring lines and spread remain the same as for the catenary system, i.e. four clusters of four lines, see figure 3.5. The platform chain and bottom chain segments are set equal to the platform chain for the catenary system. The mid segment is altered to a polyester rope, which spans almost the entire water column. The specifics can be seen in table 3.4.

Segment	Segment type	Diameter	Length	E-modulus	Weight in water
1	Chain	145 [mm]	100 [m]	36900 [MPa]	3,587 [kN/m]
2	Polyester rope	263 [mm]	1922 [m]	5086 [MPa]	0.1089 [kN/m]
3	Chain	145 [mm]	100 [m]	36900 [MPa]	3,587 [kN/m]

TABLE 3.4: Taut-leg system

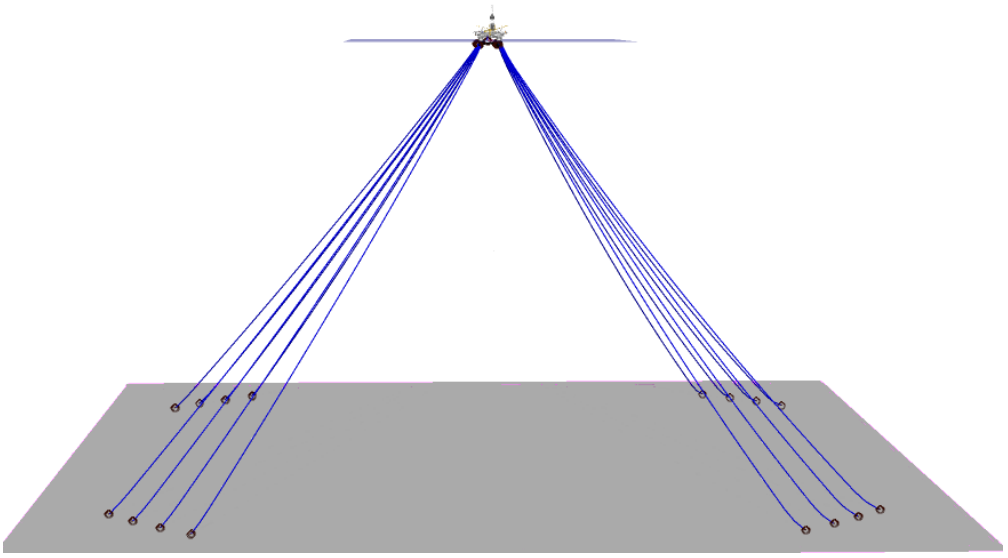

FIGURE 3.5: Taut-leg mooring system

3.3 Acceptance Criteria for Norwegian Continental Shelf

The mooring design code for the Norwegian Continental Shelf (NCS) is design against overload according to three limit states. These limit states shall ensure no failure of the mooring lines. The limit states are

- Ultimate limit state(ULS)
- Accidental limit state(ALS)
- Fatigue limit state(FLS)

Ultimate limit state is design against overload for an *intact* mooring system in extreme weather. Accidental limit state is design against overload for a *damaged* mooring system in extreme weather. Fatigue limit state is design against fatigue failure taking all possible sea states into account. This thesis will not investigate FLS.

For ULS and ALS, the code format demands that the minimum breaking strength (MBS) of a mooring line is higher than the most probable highest tension T_{MPM} of the same mooring line, by a factor called the safety factor (sf), see equation 3.1.

$$MBS \geq T_{MPM} \cdot sf \tag{3.1}$$

The most probable max is established by two separate software tools, both presented in chapter 4, where the vessel and mooring system are subjected to the worst 100 year sea state.

The safety factor is different for ULS and ALS, and for different regions of the world.

Weather Condition	Intact (ULS)	One Line Failure	Two Line Failure
100 year return period	2.2	1.5	N/A
10 year return period	N/A	N/A	1.5

TABLE 3.5: Requirement to safety factors for production units on NCS,(ISO Standard, 2013)

As seen in table 3.5, the safety factor for ULS is required to be 2.2 or higher, and for ALS it is required to be 1.5 or higher.

When the MPM is found and the correct sf is applied, mooring line components with higher MBS than the product of sf and MPM are chosen.

3.4 Environment

The environmental forces will be described next. The simulation is based on a typical 100-year condition. Meaning that the waves and wind will be the expected worst for 100 years, and the current will be the expected worst for 10 years. This is because it is too conservative to assume the worst current will coincide with the worst wind and waves.

The environment conditions used throughout the comparison between MIMOSA and SIMO/RIFLEX are presented in tables 3.6, 3.7, and 3.8. For the accidental limit state analysis, the same environment was used, but with a heading of 45 degrees, as this will primarily affect only one mooring line cluster, and is therefore assumed to be more severe with respect to a progressive failure.

All environmental data is taken from the Metocean Design Basis for Heidrun, see (DNV GL, 2004).

Waves

The waves generated are based on the Torsethaugen double peaked spectrum, which only requires three input parameters. These are significant wave height, peak period, and heading. The significant wave height and corresponding peak period are taken for an extreme 3-hour seastate, with a 100-year return period.

Significant Wave height	Peak Period	Heading
16 [m]	18.2 [s]	0 [Degrees]

Table 3.6: Wave conditions used for the analysis

The worst sea state may not be the sea state with the highest significant waveheight and corresponding peak period, but a point along the contourline in figure 3.6. (Stendal, 2014) shows that a point with a slightly smaller significant wave height, and a smaller peak period, gives a higher load. Since this thesis doesn't include a design check, the highest waveheight and corresponding peak period will be used throughout the analysis.

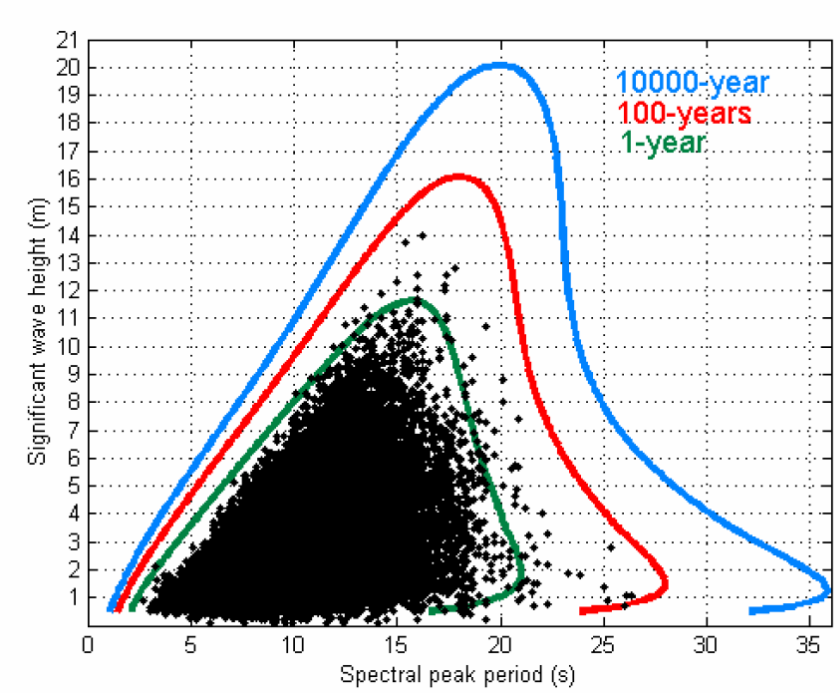

FIGURE 3.6: Contourplot for extreme value waves, (DNV GL, 2004)

Wind

The wind generated is based on the NPD/ISO spectrum, and the input parameters are mean wind speed, reference height for the mean wind speed, and heading. The mean wind speed is taken as the 1-hour mean extreme wind speed, with a 100-year return period.

Mean Wind Speed	Reference Height	Heading
36 $[\frac{m}{s}]$	10 [m]	0 [Degrees]

TABLE 3.7: Wind conditions used for the analysis

Current

The current has no spectrum, but can be specified as a depth profile. In the analyses, the current is specified to have a constant value from the surface to 20 meter depth, and be zero below 20 meters. This is since MIMOSA doesn't include drag forces from current on mooring lines, hence there should not be drag forces from current on the mooring lines in the RIFLEX analysis either.

The static current speed is taken as the 10-minutes extreme current speed at the surface with a 10-year return period.

Mean Current Speed	Heading
0.94 $[\frac{m}{s}]$	0 [Degrees]

TABLE 3.8: Current conditions used for the analysis

3.5 Software

In this chapter the software used in the analyses will be presented briefly.

MIMOSA

Mimosa is a frequency domain program, developed by MARINTEK and supported by DNV GL. It is tailor made for mooring analysis, and requires input files for the vessel and the mooring system. For further information, please see (Marintek, 2012).

Coupled SIMO/RIFLEX

SIMO is a time domain analysis tool for marine operations. RIFLEX is a time domain finite element method program for slender marine systems, such as risers and mooring lines. They can operated separately, but can also be used as a coupled model. SIMA is a graphical user interface for both SIMO and RIFLEX, for further information, please see (Marintek, 2009) and (Marintek, 2014).

Chapter 4

Numerical Simulation

This thesis researches two separate analysis cases. The first is a comparison between time and frequency domain, by using the software tools presented in chapter 3.5. The latter is an analysis of a damaged mooring system, i.e. with one mooring line broken, analysed in time domain.

4.1 Comparison of Time and Frequency Domain

There are two leading methods to perform a dynamic analysis for marine operations, the time domain and the frequency domain methods. It is therefore interesting to compare them, and see which results they give.

4.1.1 Input Verification and Sources of Errors

The first analysis case was analysed for two mooring systems, both presented in chapter 3. Before any analyses could be performed, a tedious comparison was made between the input files, to try to locate error sources and reduce the discrepancies between the results from MIMOSA and SIMO/RIFLEX.

To do these comparisons, it was important to keep in mind differences in definition of axes and units between the software tools.

The RAOs were compared for all six DOFs graphically. The translatory motion RAOs, exemplified by surge motion in figures A.2 and 3.1, are comparable without any interpretation.

For the angular motion RAOs, exemplified by the pitch motion in figures A.9 and A.10, some interpretation is needed. The MIMOSA angular RAOs are made dimensionless by dividing with the wave number, while the SIMO angular RAOs are not. The equality between the plots has been verified by also expressing the SIMO angular RAOs dimensionless. The rest of the plots can be seen in Appendix A.

The current and wind coefficients were also compared graphically, and can be seen in Appendix A. Some interpretation is needed here as well. The units are different, i.e SIMO uses [kN] where MIMOSA uses [N]. For the wind coefficients, there is a 180^o shift, and the relative angle between wind and heading is defined as positive for clockwise rotation for MIMOSA, and counter-clockwise for SIMO. For the current coefficients, there is no shift, but the relative angle between current and heading is defined as for wind. With these alterations in mind, the coefficients are correct.

When the low frequency motions are calculated in MIMOSA, only the three in-plane DOFs surge, sway and yaw are calculated. This leads to an error, e.g. the motion in x-direction will get a contribution from the pitch and roll motion, see equation 2.4, but this will not be accounted for in MIMOSA. This will only be a problem for the pitch motion, as the environmental forces have a zero degree heading in the analysis, and hence there will be virtually no roll motion.

The restoring force curves and the line characteristics have been compared. They are found easily in MIMOSA by offsetting the vessel a given distance, and the forces will be given as output. For SIMO/RIFLEX, an external force has to be specified without any environmental forces, and the resulting offset is given as output. Both the restoring force curves and the line characteristics are given in chapter 5.

When exporting the MIMOSA model to a RIFLEX model for the deep water taut-leg system, something went wrong, and the SIMO/RIFLEX analyses give results which are incorrect. A lot of time and effort was put into solving these problems, but the problems remain unsolved. The focus on the comparison of time and frequency domain

has therefore been shifted, and the subsequent comparison has only been carried out for the catenary mooring system.

4.1.2 Analysis Procedure

Once all the input had been verified, the system was analysed. To compare the TD and FD, it was natural to compare the following results

- Most Probable Max Tension in the Mooring Lines
- Most Probable Max Surge Motion
- Mean Tension in the Mooring Lines
- Static External Forces
- Static Offset
- Surge Standard Deviation
- Tension Standard Deviation

For the time domain analysis in SIMO/RIFLEX, 20 simulations were performed for the same environmental forces, but with different seed numbers. For the frequency domain analysis in MIMOSA, only one analysis was needed, since it gives all the statistical properties directly. The results are obtained easily with the MIMOSA software, while for the SIMO/RIFLEX software, some post-processing and filtering are needed. This will be described next.

The most probable max surge motion was found by choosing the maximum surge motion for each time series generated, and make a Gumbel distribution with a 0.37 chance of exceedance.

The most probable max tension in the mooring lines was found similarly as the most probable max surge motion. This was done for all 16 mooring lines.

A sensitivity study was made for the Gumbel distribution, where the number of analyses was varied. This was done to see if the values for most probable max tension would stabilize for 20 analyses.

The mean tension was found by taking the mean tension for each of the 20 simulations, and then taking the mean of these 20 samples. This was also done for all 16 mooring lines.

The static external forces are given directly as output for both MIMOSA and SIMO/RIFLEX.

The static offset is found easily in both MIMOSA and SIMO/RIFLEX. There is only need for one analysis in time domain as well, since the static offset is equal regardless of seed number.

To find the low frequency surge standard deviation in SIMO/RIFLEX, the time series signal must be filtered by a low-pass filter. The cut-off frequency determined what frequencies that will pass through. To get the LF motion, a cut-off frequency of 0,0333 [Hz] was used, which corresponds to a period of 30 seconds.

The wave frequency standard deviation was found by filtering with a high-pass filter. The cut-off frequency sets the lower limit for what frequency that will pass the filter. To get the WF motion, a cut-off frequency of 0,0333 [Hz] was used.

To find the combined SD from the LF and WF contributions in MIMOSA, equation 4.1, adopted from equations in (Leira, 2010), was used.

$$\sigma_{total} = \sqrt{\sigma_{LF}^2 + \sigma_{WF}^2 + 2\rho \cdot \sigma_{LF} \cdot \sigma_{WF}} \tag{4.1}$$

where ρ is a correlation factor, in the range [-1,1], and is assumed to be zero in this calculation.

4.2 Accidental Limit States

4.2.1 Introduction

There are too many incidents occurring both in Norwegian and international waters related to mooring line failures. With such a high failure frequency, it is interesting to explore the possibility of a progressive collapse of a mooring system. To do this, one

line will be broken at the beginning of a 3 hour storm, and the subsequent motions and resulting tensions will be analysed.

After a mooring line breaks, the floating vessel will experience transient oscillatory motions before settling at a new equilibrium position. The transient condition (overshooting beyond the new equilibrium position) may, in some instances, govern the mooring design, (Kwan, 1991).

A broken mooring line may take six months to replace, (Larsen, 2015). It is therefore likely that a vessel with a line broken will experience rough weather conditions.

It is of interest to see whether or not a second line will experience a load higher than the MBS. And if it does, when the highest tension will occur. This could either be in the transient motion phase, or it could be after the vessel has reached the new equilibrium position. If a second mooring line is in jeopardy, it is better if the analyses show it will happen after the transient motion phase, as this gives time to readjust the mooring system and possibly avoid another broken mooring line, (Larsen, 2015). This will be explored further by analysing the time series, and see how the mooring line tension behaves in the transient motion phase, after one line is broken.

Furthermore, a mooring line could be damaged in some way, resulting in a lower MBS than anticipated. If this is the case for the second most loaded mooring line, and the most loaded mooring line fails, there is a risk of a progressive collapse.

There are many failure mechanisms responsible for a mooring line failure. These are presented as a fault tree in figure 4.1. The numbers in table 4.1 show the number of mooring line failures due to the specific failure mechanisms for the NCS between 2000 and 2013. All numbers are taken from (Brindley and Brandsæter, 2015).

4.2.2 Analysis Procedure

The mooring system described in chapter 3 has been analysed in SIMO/RIFLEX for the same conditions with 20 different seed numbers. After 600 seconds, the most loaded mooring line has been cut, and the analyses have continued for another 3 hours.

For the condition with the exact same seed numbers, the analyses have also been performed without a broken line. This is to compare how the mean and max tensions and

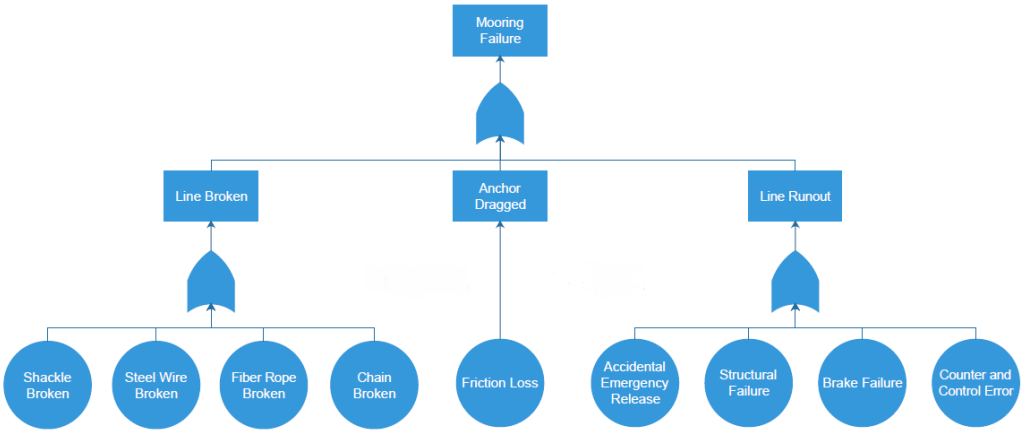

FIGURE 4.1: Fault tree

Intermediate Event	Basic Event	Number of Failures
Line Broken	Shackle Broken	3
	Steel Wire Broken	3
	Fiber Rope Broken	5
	Chain Broken	14
Anchor Dragged	Friction Loss	3
Line Runout	Accidental Emergency Release	5
	Structural Failure	3
	Brake Failure	3
	Counter and Control Error	2
	Unknown Cause	2

TABLE 4.1: Failure mechanisms, (Brindley and Brandsæter, 2015)

offsets change with a broken line. With an intact system, each of the four mooring lines in the cluster will have to account for approximately 25 % of the total load, while with one mooring line broken, the three remaining mooring lines in the cluster, will have to account for approximately 33 % each. It will be explored if the mean and max tension will increase with 33 %, or if there are some dynamic effects increasing or decreasing the values.

To induce a second mooring line failure, either the MBS could be reduced or the environmental forces could be increased. In order to avoid running too many simulations, the probability of a second mooring line failure will be presented as a function of MBS, where the MBS will be reduced in the post-processor. This will give the probability of failure of a second mooring line, given failure of the first mooring line, as a function of MBS. The MBS designed for, is decided by taking the Gumbel distribution of the

maximum mooring line tensions for each condition, to find the most probable maximum tension, and multiply this number by the safety factor, which is 2.2.

Another set of analyses was performed, where the most loaded line was cut at different times in the vicinity of the highest tension recorded for all 20 seed numbers. This was done to explore if the exact moment of failure would affect the maximum tension. These results were then compared with the same seed number, where the line was cut at the beginning of the simulation. The line was cut 12 times, all in the vicinity of the highest tension recorded, among them the moment with the highest tension and the moment with the highest velocity. These results are presented in figure 5.15.

Chapter 5

Results and Discussion

The results of the two analysis cases will be given next. The results will be discussed immediately after they have been presented.

5.1 Comparison of Time and Frequency Domain

5.1.1 Static Motion Comparison

When comparing the systems analysed statically, equation 2.5 simplifies to only the load and the stiffness terms. To check compliance, the restoring forces, the static external forces and equilibrium position have been compared.

The comparison of restoring forces shows almost the exact same curve, at least for offsets smaller than 40 meters. Based on this, the mooring system stiffness is assumed to be equal.

The comparison of line characteristics for the most loaded line also shows a good compliance, with slightly higher tensions for the MIMOSA model.

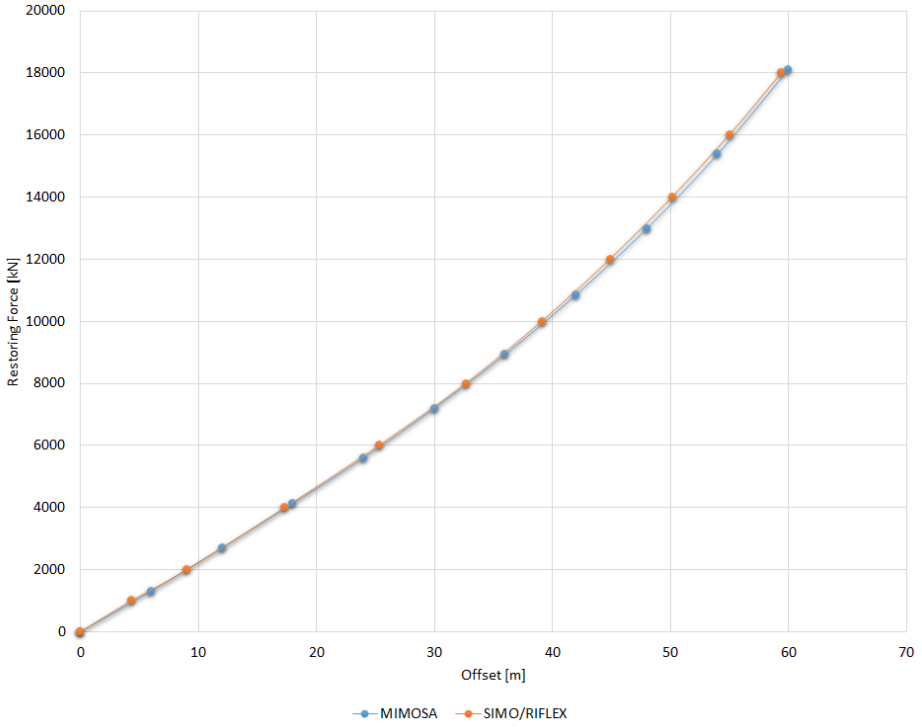

FIGURE 5.1: Restoring forces as function of offset

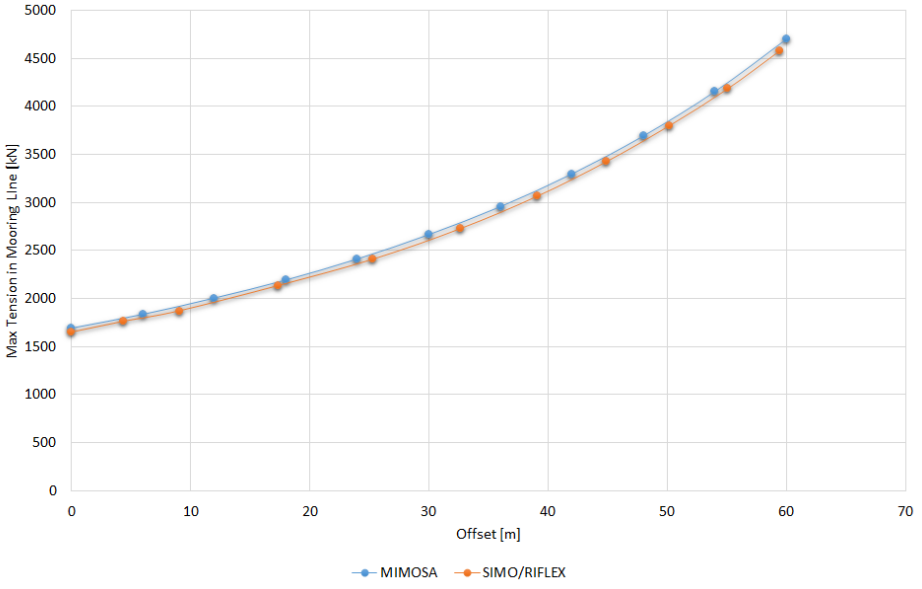

FIGURE 5.2: Comparison of line characteristics

The comparison of static external forces in figure 5.3 shows there is a good compliance between MIMOSA and SIMO. However, the current forces differ by roughly 10 %, which seems too much, given the relatively simple equation for the static current force, which can be seen in equation 2.15. A hand calculation was performed to compare with the SIMO and MIMOSA results, and can be seen in table 5.1

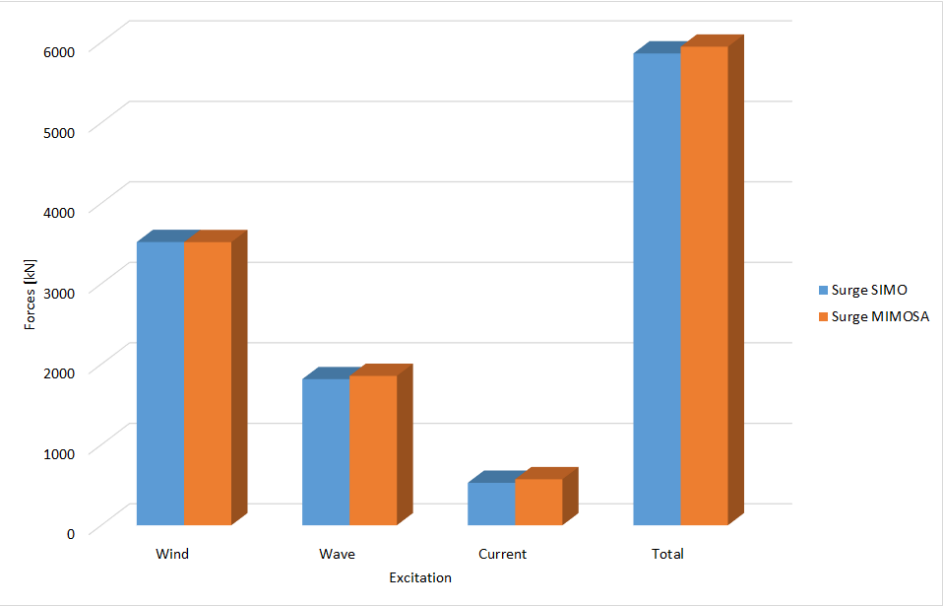

FIGURE 5.3: Comparison of static external forces

	Mimosa	SIMO/RIFLEX	Hand Calculation
Current Force [kN]	572,2	527,7	569

TABLE 5.1: Comparison of current forces

The hand calculation shows that SIMO/RIFLEX estimates the current force as too low. This will lead to a small error, but will not be further investigated, as the time doesn't allow it and the total environmental force deviation is only 1.43%.

With the results of restoring forces and static external forces, it is reasonable to assume that the static offset will yield similar results for the two models, which is true, and can be seen in table 5.2

	MIMOSA	SIMO/RIFLEX
Static Offset [m]	25,34	24,47

TABLE 5.2: Static offset in surge

The static offset is slightly lower for SIMO/RIFLEX, which is probably due to the decreased current force value in SIMO/RIFLEX.

5.1.2 Dynamic Motion Comparison

The dynamic motion comparison is more challenging, since MIMOSA separates the motions into low and wave frequency, while SIMO/RIFLEX does not. This makes the

comparison more difficult, but the contributions have been compared nonetheless. To negate this issue, the MIMOSA contributions have to be combined, or the SIMO/RIFLEX contribution has to be filtered, to give values for LF and WF. The standard deviation (SD) of the motion is compared for the dynamic motion. The surge LF SD, and the surge, heave and pitch WF SD are given in table 5.3, where the SIMO/RIFLEX contributions have been filtered.

	MIMOSA	SIMO/RIFLEX	Deviation
Surge LF [m]	4.84	4.53	6.84 %
Surge WF [m]	2.69	2.31	16.4 %
Heave WF [m]	2.27	2.05	10.7%
Pitch WF [Deg]	1.38	1.39	0.7%

TABLE 5.3: Standard deviation filtered

The SD for the LF surge motion is proportional to the square root of the force spectrum at resonance frequency, divided by the product of the stiffness and the damping, seen in equation 5.1, (Faltinsen, 1990).

$$\sigma_{LF} \sim \sqrt{\frac{S_F(\mu) \cdot \pi}{2k \cdot c}} \tag{5.1}$$

The force spectrum and stiffness have already been verified, which only leaves the damping. The LF SD for SIMO/RIFLEX is smaller, i.e the damping is larger. This is a reasonable result, as the dynamic damping from the drag forces on the mooring lines, described in section 2.2.2, is not included for the MIMOSA analysis.

The WF surge and heave SD are larger for MIMOSA than for SIMO/RIFLEX. The deviation is substantial, and is assumed to be because of problems with the filtering process in SIMO/RIFLEX.

For the combination of contributions from MIMOSA comparison, the deviation of SD in surge is much smaller, see table 5.4.

	MIMOSA	SIMO/RIFLEX	Deviation
Standard Deviaton Surge	5.54	5.32	4.1%

TABLE 5.4: Standard deviation combined

The estimated max surge motion in MIMOSA is calculated according to equation 2.37, and the results are given in table 5.5

Equilibrium Position		25.34
LF	Max amplitude	20.61
	Significant amplitude	9.67
WF	Max amplitude	10.10
	Significant amplitude	5.37
Total	Equilibrium + Max LF + Sign WF	51.32

TABLE 5.5: MIMOSA surge motion

The estimated max surge motion in SIMO/RIFLEX is calculated directly. It is taken as the most probable max surge motion, based on a Gumbel distribution for 20 simulations. The most probable max surge motion is seen in table 5.6.

Most Probable Max Surge Motion	49.21 [m]

TABLE 5.6: Most probable max surge motion, taken from SIMO/RIFLEX

The results are acceptable, with the result from MIMOSA as the conservative value, which is in accordance with theory.

Furthermore, the relationship between surge maximum amplitude and surge SD has been investigated. The relationship expresses if the process is Gaussian distributed or not.

	MIMOSA	SIMO/RIFLEX
Maximum Surge Amplitude	25.98	24.74
Standard Deviation	5.54	5.32
Max/SD	4.69	4.65

TABLE 5.7: Relationship between surge maximum amplitude and standard deviation

With a Gaussian process, the relationship should be equal to $\sqrt{2ln(N)}$, where N is the number of samples. For surge motion in a 3 hour period, the relationship should be approximately 3, i.e. the surge motion can not be said to be a Gaussian process.

5.1.3 Tension Comparison

For the tension, there are several parameters worth comparing, of course the maximum tension and the mean tension are among them, but the SD is also a good parameter. To compare the SD, either the LF and WF contributions from MIMOSA have to be combined, or the SIMO/RIFLEX contribution has to be filtered. The following plots present the results for both methods.

The SIMO/RIFLEX LF and WF SD contributions are obtained by filtering, presented in chapter 4.1.2.

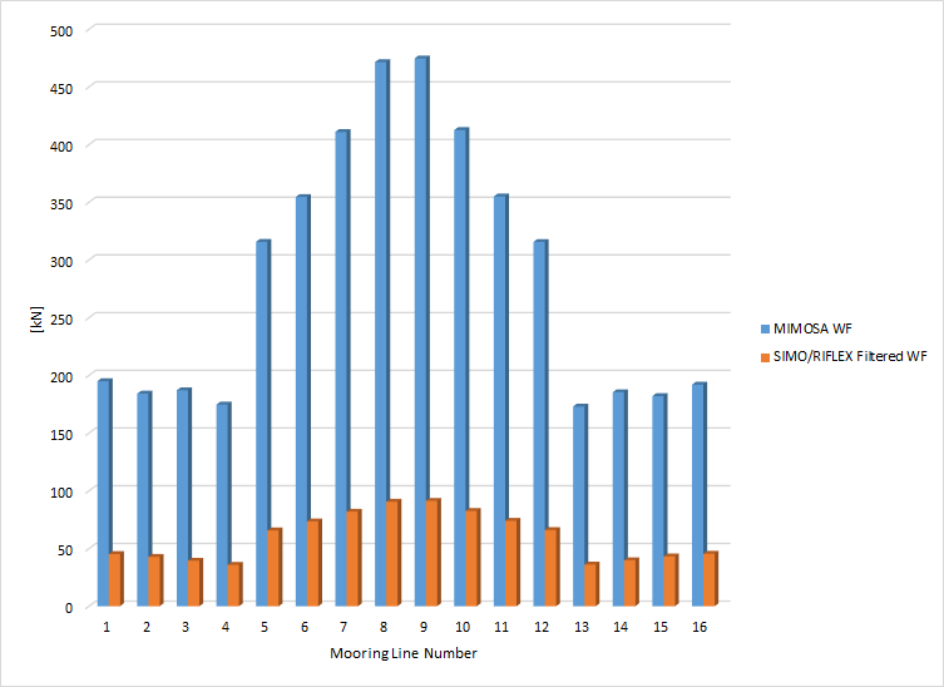

FIGURE 5.4: Wave frequency standard deviation

The wave frequency tension SD is several times higher for MIMOSA than for SIMO/RIFLEX. This is believed to result from the the filtering process and the way the programs calculate tension. For MIMOSA, the wave frequency motion is calculated around X_{base}, seen in figure 2.15, which makes the tension much higher than for SIMO/RIFLEX.

For the low frequency tension SD, seen in figure 5.5, it is the other way around, and the SD is higher for SIMO/RIFLEX. It is believed that there are some problems with splitting the time domain signal into two contributions, as presented. The low pass filter is not able to completely filter out the WF contribution, therefore the WF contribution from SIMO/RIFLEX is too low, and the LF contribution from SIMO/RIFLEX is too high. By combining the contributions from frequency domain instead, the results are much better, as can be seen in figure 5.6. The MIMOSA SD is estimated based on the method presented in chapter 4.1.2. MIMOSA still gives a conservative value compared to SIMO/RIFLEX, which is expected.

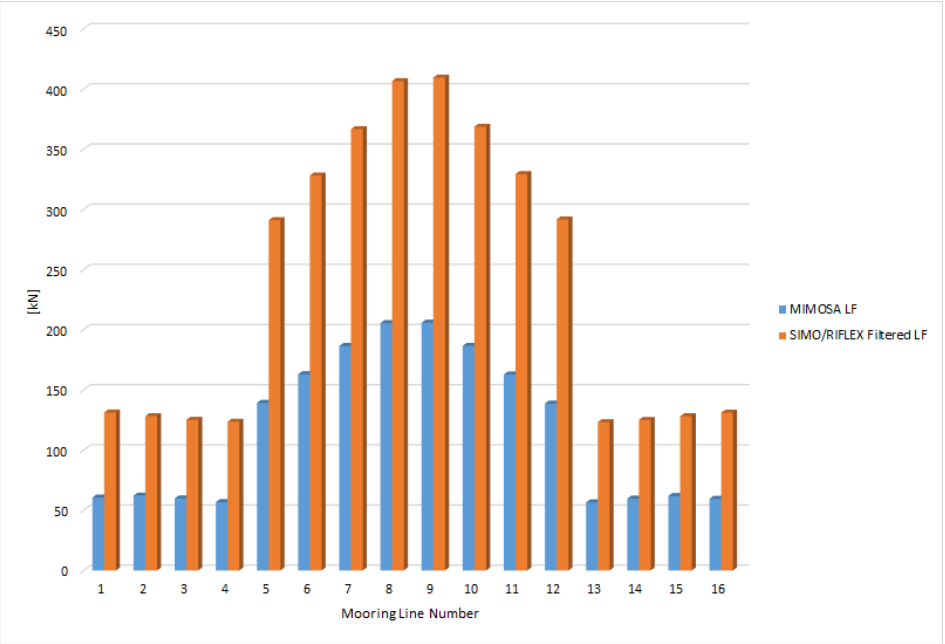

FIGURE 5.5: Low frequency standard deviation

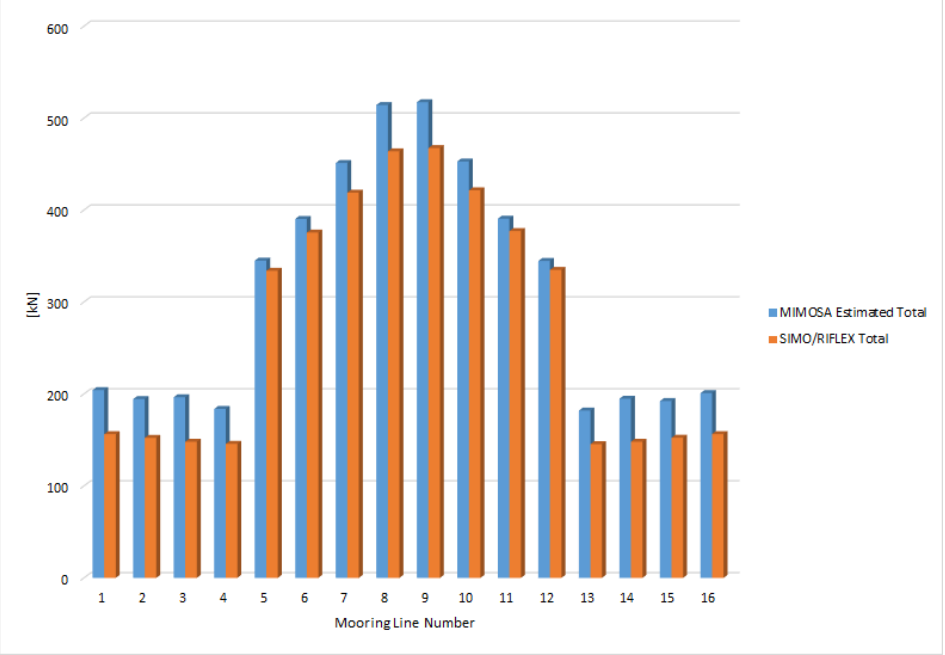

FIGURE 5.6: Total standard deviation

To find the most probable max tension in SIMO/RIFLEX, 20 simulations were performed, and the maximum tension in each simulation was used in a Gumbel distribution, to find the most probable maximum tension. The results for each line can be seen for both MIMOSA and SIMO/RIFLEX in figure 5.7.

For the windward lines (line 5-12), which are of primary interest, MIMOSA gives higher tensions than SIMO/RIFLEX. The most loaded mooring line is mooring line 9, and here the max tension is 9.4% higher for MIMOSA.

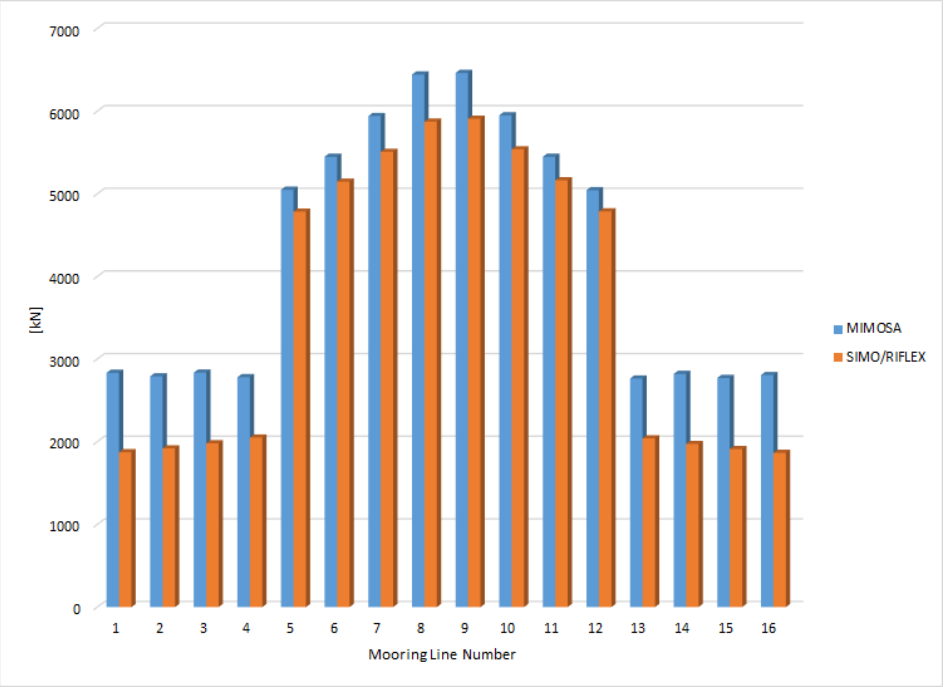

FIGURE 5.7: Most probable maximum tension for all 16 mooring lines

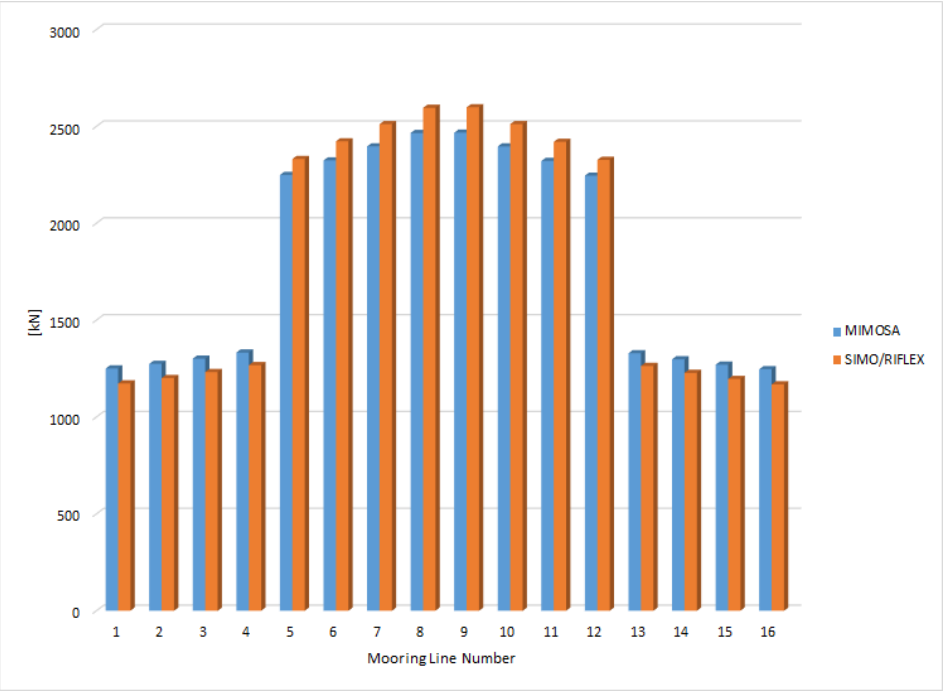

FIGURE 5.8: Comparison of mean tension for all 16 mooring lines

There is only a small deviation for mean tension in the mooring lines, with a 5.3% higher tension for the most loaded line. The mean tension is higher in SIMO/RIFLEX for windward lines, and lower for leeward lines.

The trend for the parameters investigated, shows that MIMOSA gives conservative values compared to SIMO/RIFLEX. The results from both methods are reasonable, but MIMOSA gives conservative values due to e.g. linearisation and omitting damping contributions. The analysis was a typical 100-year return period storm, where the non-linearities cannot be properly captured by MIMOSA. An analysis in intermediate sea state is better suited for MIMOSA.

5.2 Accidental Limit State

With the environmental forces directed towards the cluster with windward lines 5,6,7 and 8, a preliminary analysis show that line number 6 is the most loaded. Line 6 is therefore chosen as the line to be broken in the ALS analyses. The second most loaded line is line number 5, and is therefore chosen for further analysis.

5.2.1 Difference between Intact and Broken System

Figure 5.9 depicts the combined line characteristics for the leeward and windward clusters. When all the mooring lines are intact, and there are no environmental forces present, the vessel will be in equilibrium position, $x_{eq,1}$. With the presence of environmental forces, the vessel will settle at a new static offset, $\bar{x}_1$, and the mooring system will experience a corresponding restoring force, R_1, to counteract the environmental forces.

When a mooring line fails, the new equilibrium position will be $x_{eq,2}$, where the curve for the leeward cluster line characteristics intersects the curve for the broken windward line cluster characteristic. With environmental forces present, the vessel will move to a new static offset, $\bar{x}_2$, where $R_1 = R_2$.

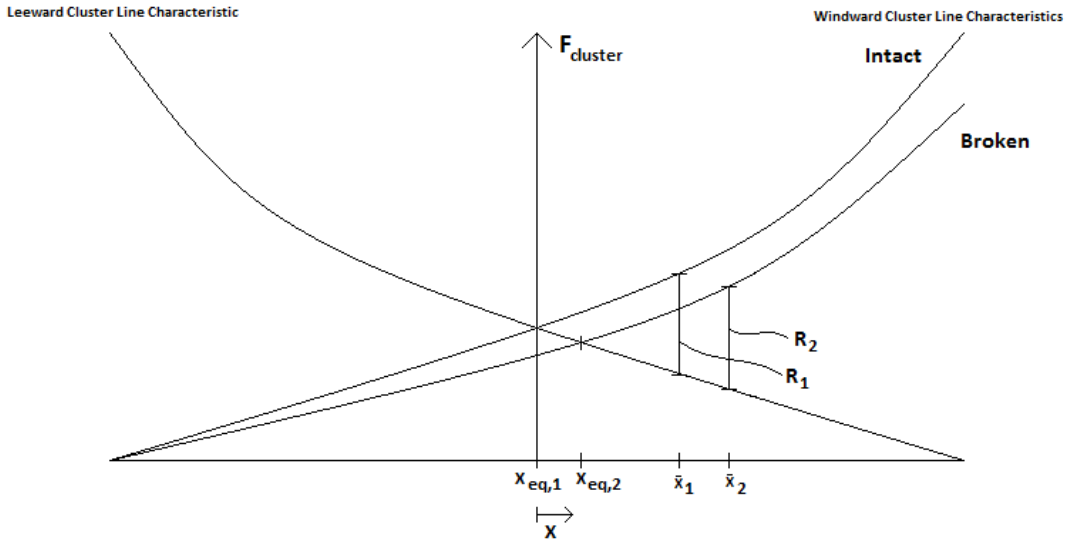

FIGURE 5.9: Change in line characteristics for a cluster, with a broken line

The vessel's dynamic motion will be around the static offset, $\bar{x}$, and the mean tension will be approximately equal to the the static tension at this offset.

The mean and max tension have been compared for the intact and broken system. The mean and max tension for all mooring lines can be seen in figures 5.10 and 5.11, respectively.

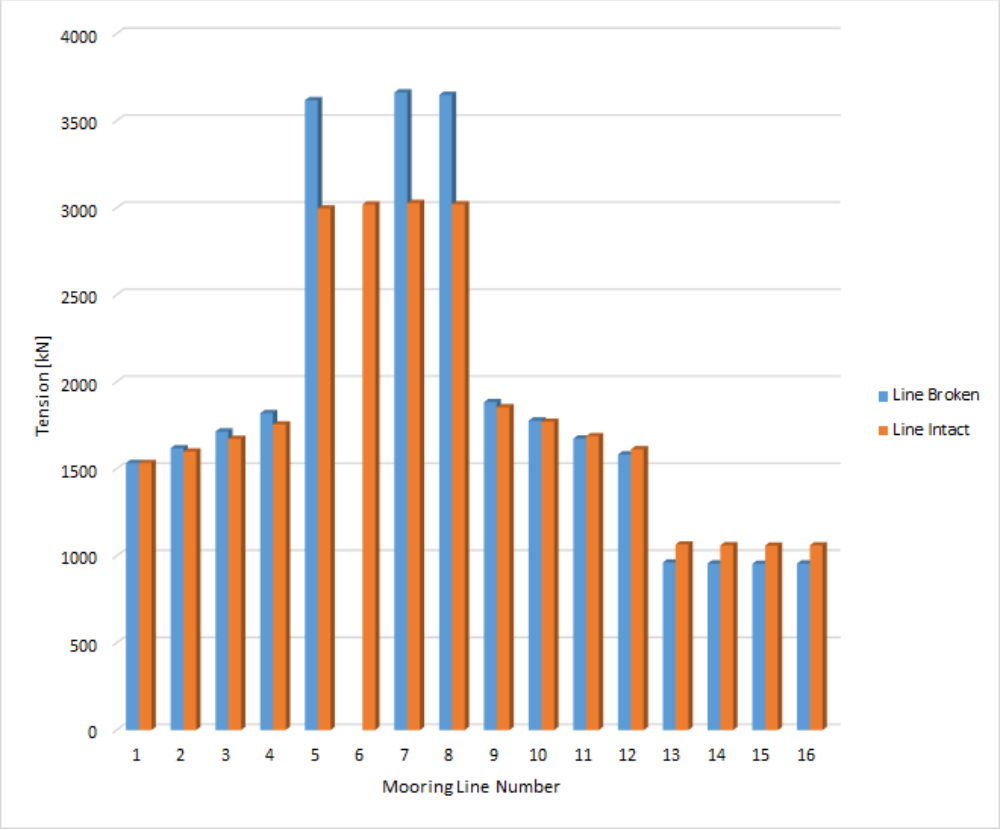

FIGURE 5.10: Mean tension for all 16 mooring lines

The mean tension in line 5, which is studied more closely, increases by 21%.

The maximum tension in line 5 increases by 25% when line 6 is broken. It is reasonable that the maximum tension will increase more than the mean tension when a mooring lines breaks. The contribution to tension from the increased offset will be the same, and for a given environmental force, the broken mooring system will be less robust, and will therefore experience a larger offset, resulting in larger tension.

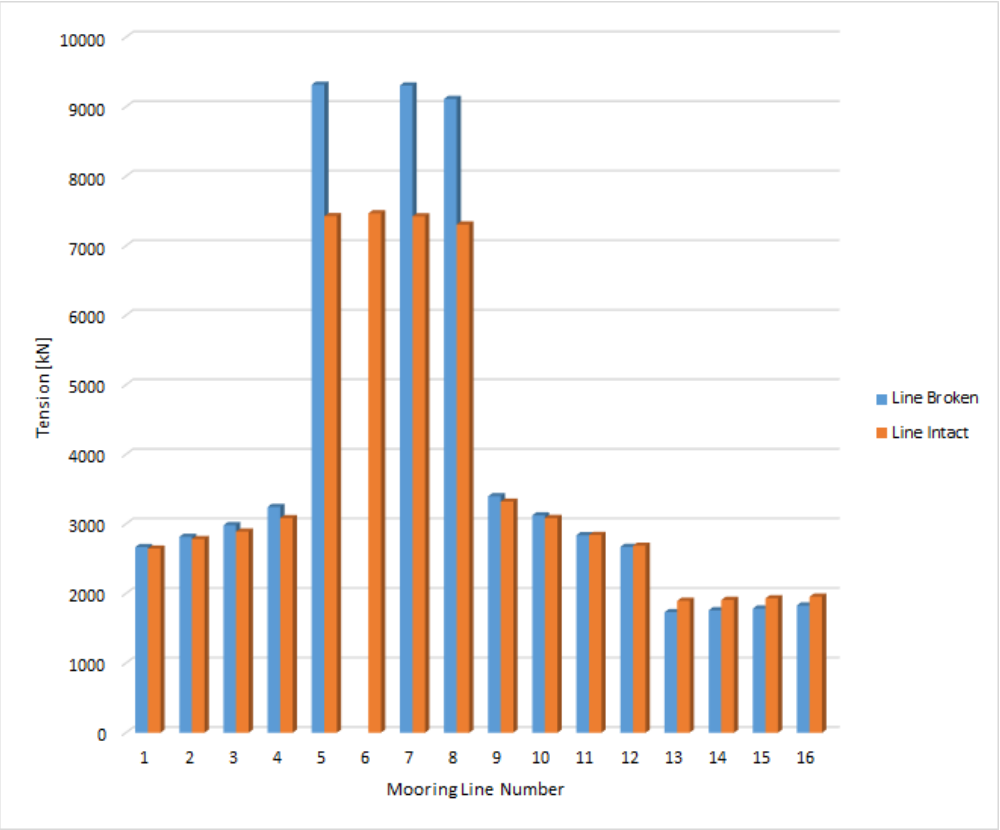

FIGURE 5.11: Max tension for all 16 mooring lines

5.2.2 Probability of Failure with one Mooring Line Broken

Figure 5.12 shows the probability density functions of the most probable maximum tension of mooring line 5. The magenta curve depicts an intact system and the red curve depicts a damaged system. Both distributions have been produced through a Gumbel distribution made in MATLAB, with the maximum tension for 20 time series as input.

The green line is the MBS, which is found in accordance with equation 3.1. The three cyan lines are 70%, 80% and 90% of the MBS.

The MBS of a chain link is assumed to be Gaussian distributed. Since a mooring line breaks when an arbitrary chain link breaks, the MBS distribution of a mooring line is a very narrow distribution, and can be assumed to be a constant value. The MBS in 5.12 is therefore given as vertical lines, not as distributions. The MBS of the mooring line is compared with the Gumbel distribution for MPM tension for the broken mooring system. The MBS of the mooring line is decreased with intervals of 5 %, and the points are plotted with the corresponding probabilities in figure 5.13.

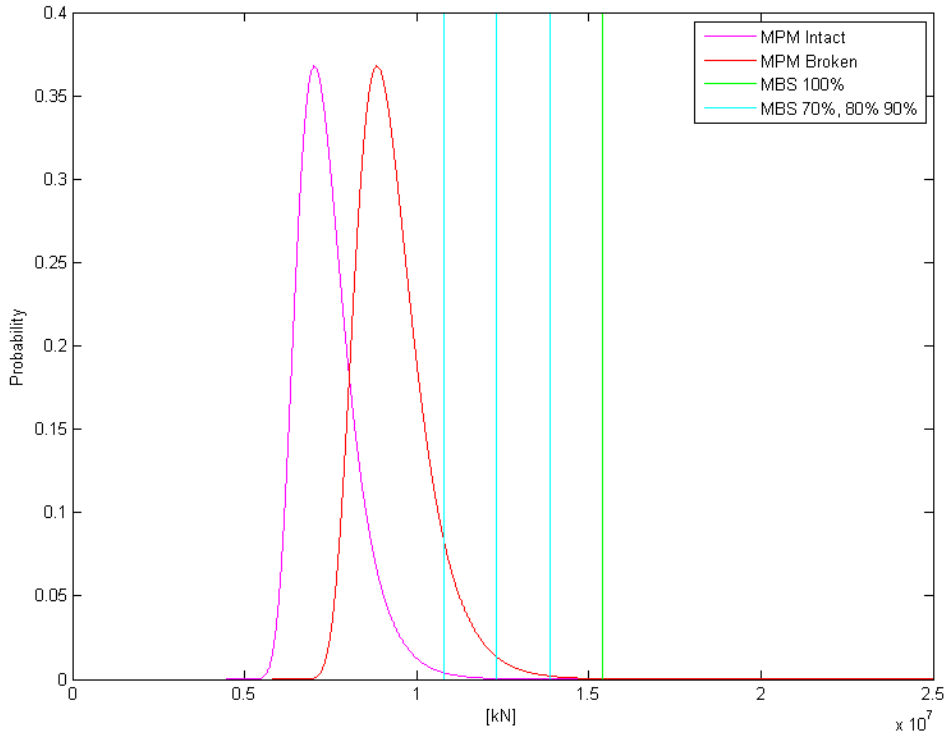

FIGURE 5.12: PDF of the most probable max tension of mooring line 5

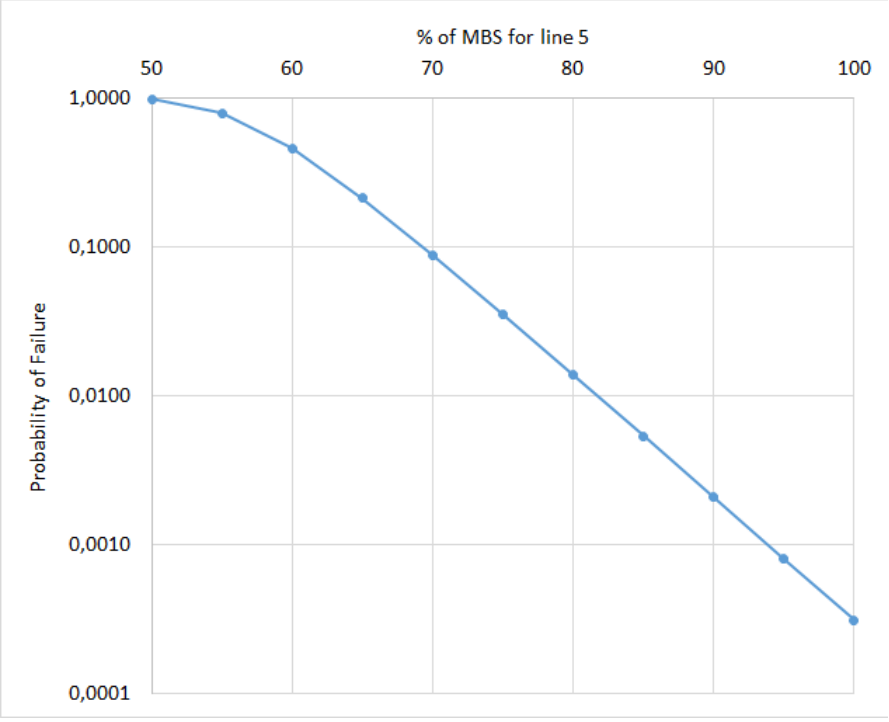

FIGURE 5.13: Probability of failure for line 5, given failure in line 6, as function of MBS for line 5

The figure illustrates the low probability of a progressive collapse, with one mooring line already broken. This is due to the very low SD of the of the MBS, and since the MBS is a conservative guaranteed value from the manufacturers. There has to be a serious degradation of the mooring line, in order for the probability to reach a dangerous level. As figure 5.13 depicts, when the MBS is degraded to 80 % MBS, there still is just 1.38 % chance of failure. If the MBS is 100% of expected, which is reasonable, there is only a 0.03% chance of failure of the second most loaded line.

5.2.3 Investigation of Time of Failure

As discussed in section 4.2, it is important to find out *when* a mooring line will fail. An investigation of the time of failure was therefore performed, to see how this would affect the maximum tension and offsets.

The largest recorded tension for the windward mooring lines, for the condition with 20 seed numbers, was for seed number 11. The time series of the tension in mooring line 5 can be seen in figure 5.14.

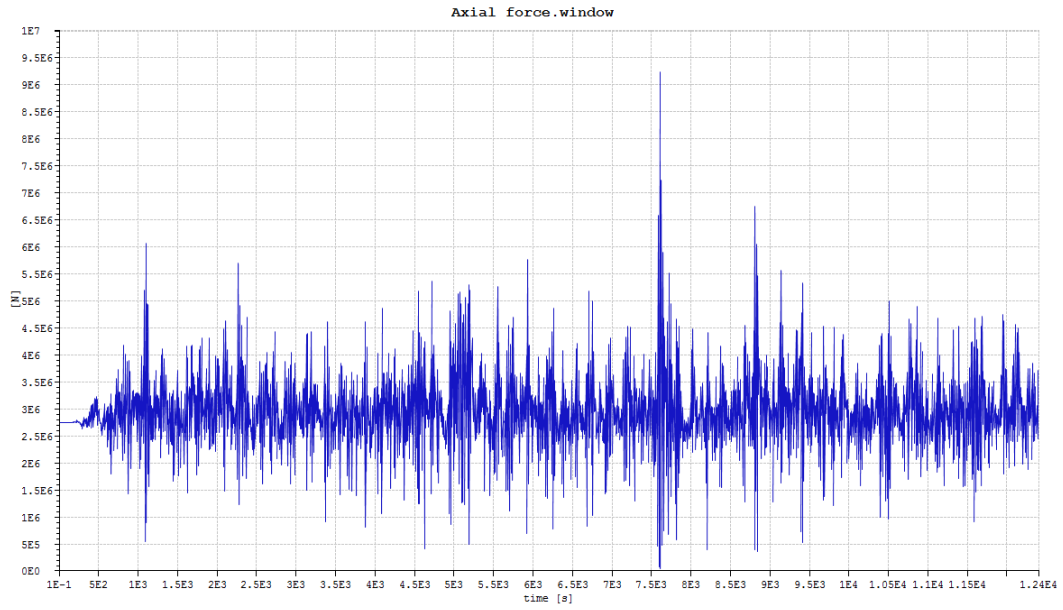

FIGURE 5.14: Time series of the tension in mooring line 5 for seed number 11

This extreme peak in tension was chosen as basis for a set of analyses where the time of failure was varied, to see what would give the highest tension and offset.

Figure 5.15 depicts the maximum tension in mooring line 5, as a function of when mooring line 6 is failing. The orange line is the maximum tension found for seed number

11, when the mooring line was cut after 600 seconds. The green line is the maximum tension found for seed number 11, with an intact system. The yellow, vertical line shows where the highest tension peak for seed number 11 occurs, which is after 7609 seconds of the simulation.

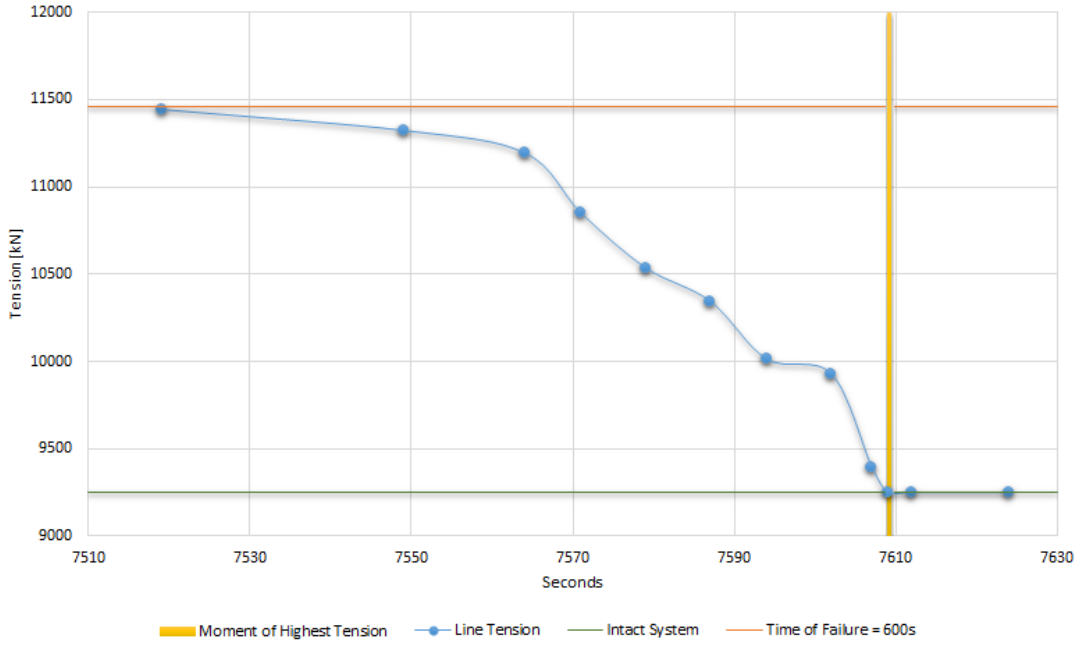

FIGURE 5.15: Max line tension as function of time of failure

Figure 5.15 shows that the maximum tension recorded for the simulation, decreases as the time of failure approaches the point of the tension peak, seen in the time series in figure 5.16. This means that no subsequent tension peaks will be higher for the remainder of the simulation, even though the mooring line is broken.

Similarly, figure 5.17 and 5.18 show the maximum surge and sway for the platform, respectively, as a function of when mooring line 6 is failing. They show that a higher offset will occur in the remainder of the simulation.

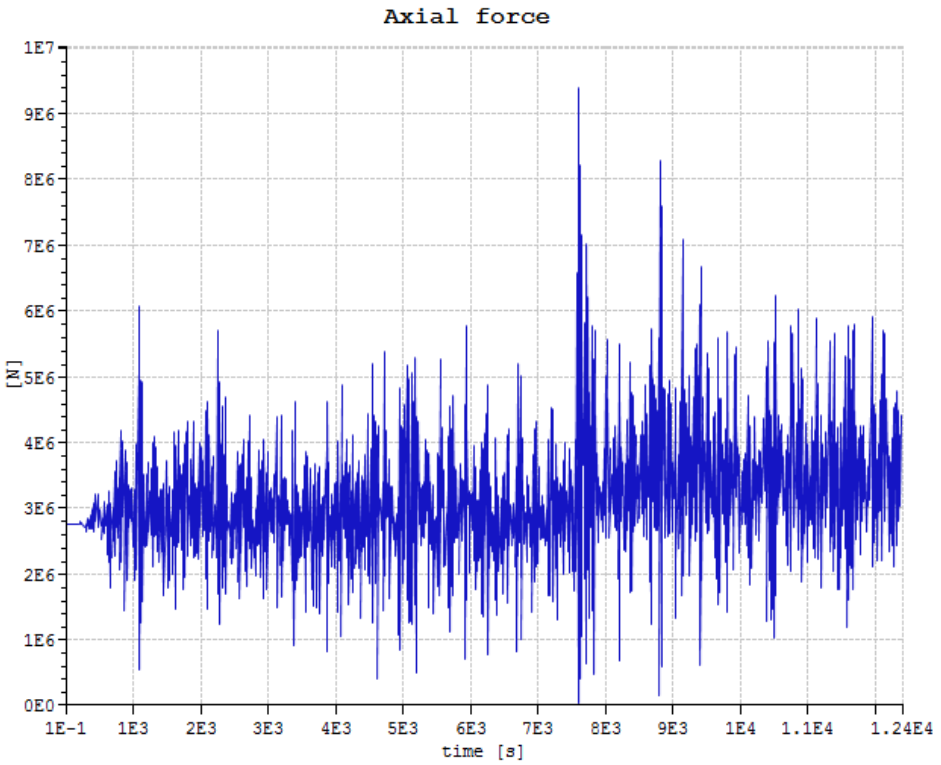

FIGURE 5.16: Tension time series for seed number 11, with line broken after 7609 seconds

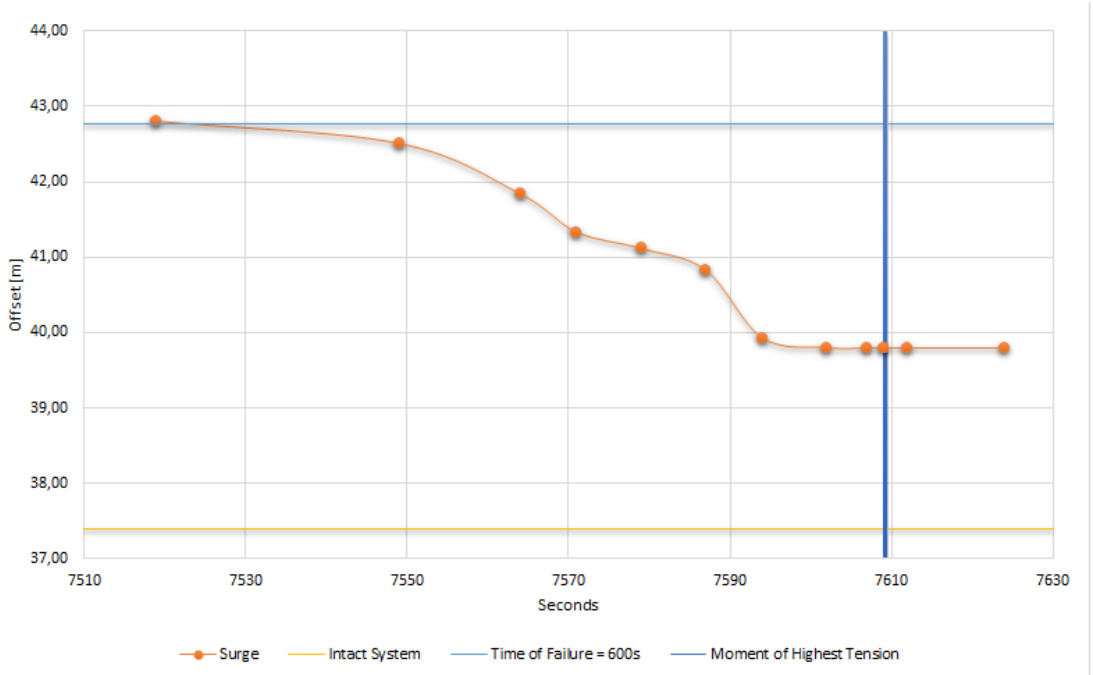

FIGURE 5.17: Maximum surge motion as function of time of failure

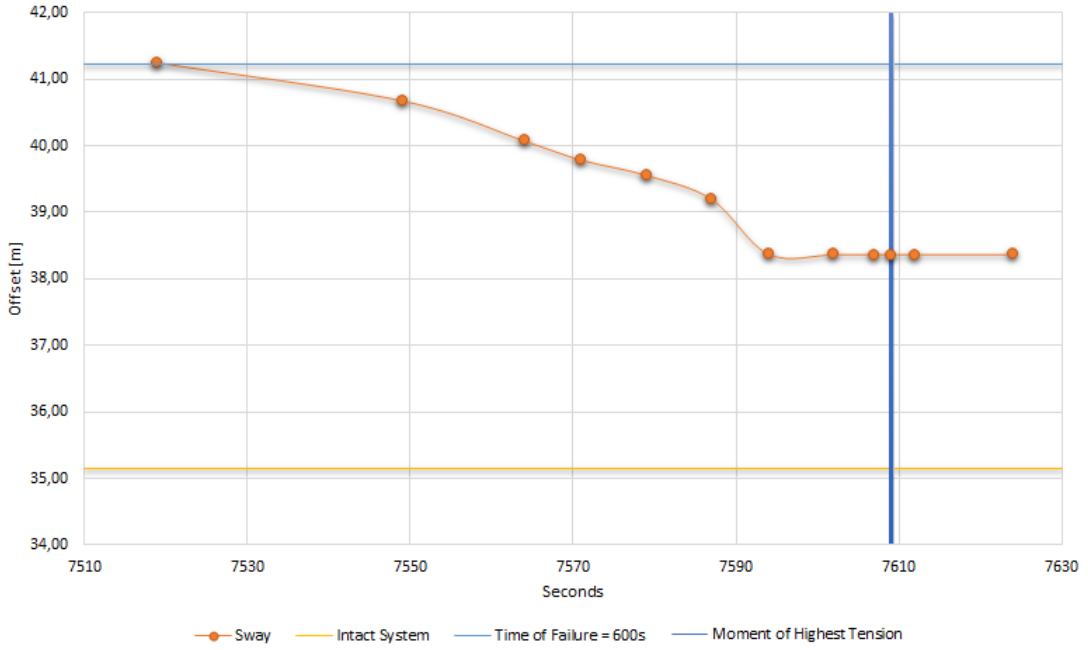

FIGURE 5.18: Maximum sway motion as function of time of failure

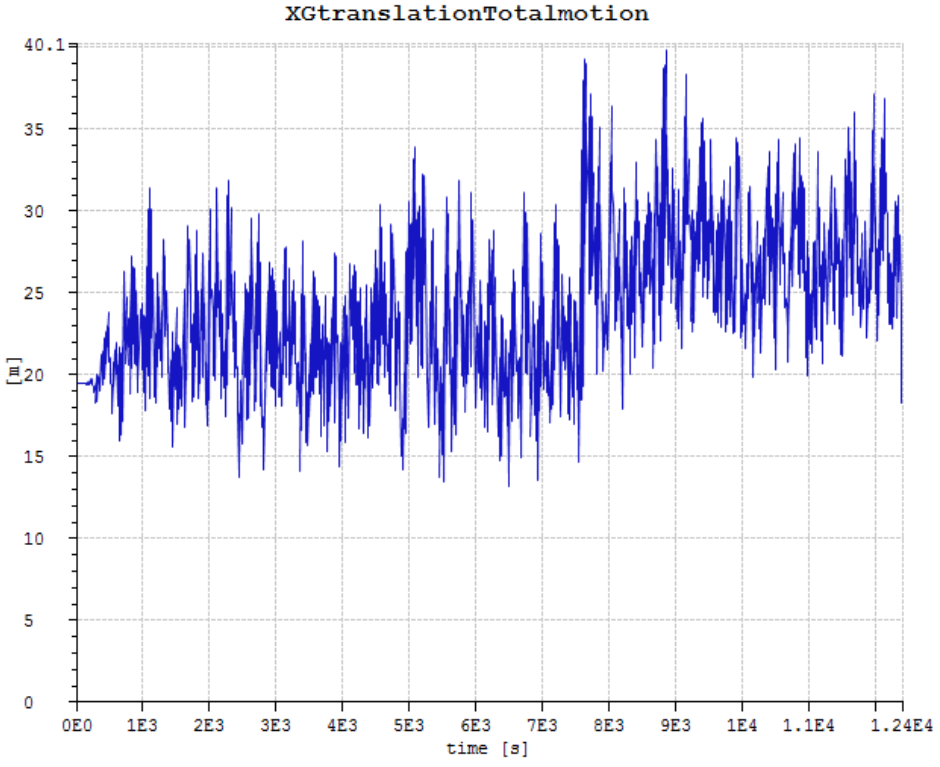

FIGURE 5.19: Surge motion time series for seed number 11, with line broken after 7609 seconds

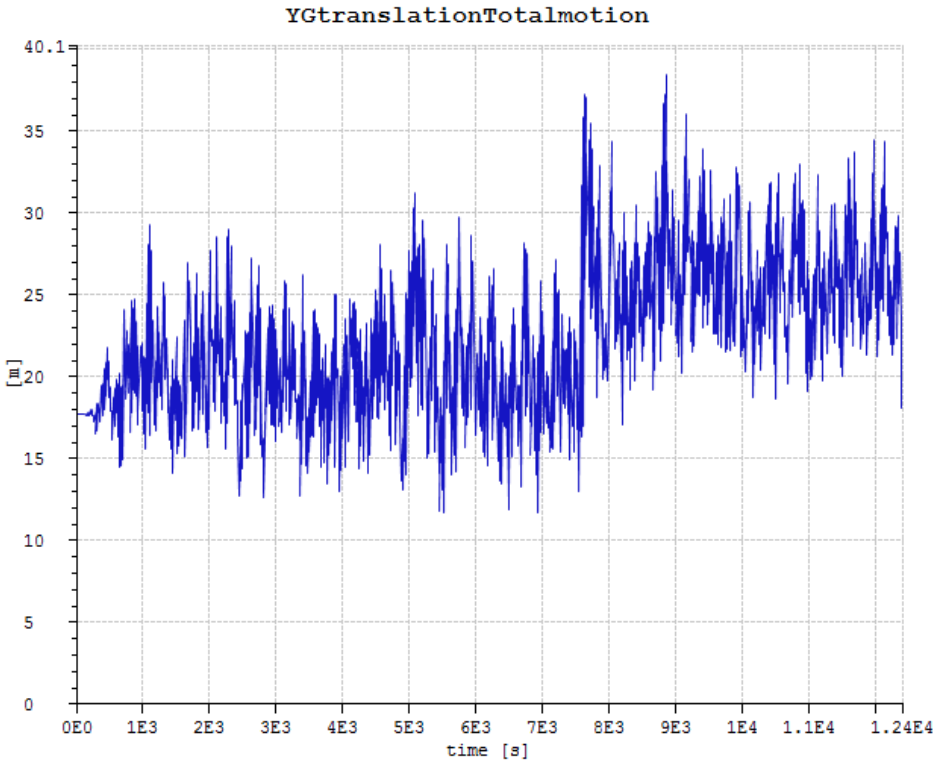

FIGURE 5.20: Sway motion time series for seed number 11, with line broken after 7609 seconds

For this specific condition, the ULS proves to be the governing design case, as the highest tension occurs when the system is still intact. With that being said, the large offset experienced after the line failure, may be critical for the integrity of risers and umbilicals.

It seems like there is a large dynamic contribution to the extreme peak tension recorded, since a subsequent higher offset, seen in figures 5.19 and 5.20, with reduced capacity, *does not* give a higher tension.

The moment with the highest tension, and therefore where the probability of failure is the highest, proves to *not* be the most critical moment to get a mooring failure. This is assumed to be since the vessel has no velocity at this moment, and is therefore pulled back towards equilibrium position, regardless of a mooring failure.

Figure 5.21 shows the time series of the tension in line 5 with the same environment, but another seed number than seed number 11. It is provided to show how another time series may look like. If the ULS design was based on this time series, the MBS would be lower. In case of a mooring line failing at the highest tension peak, subsequent

tension peaks would result in a higher tension, and thus the ALS design criterion could be governing.

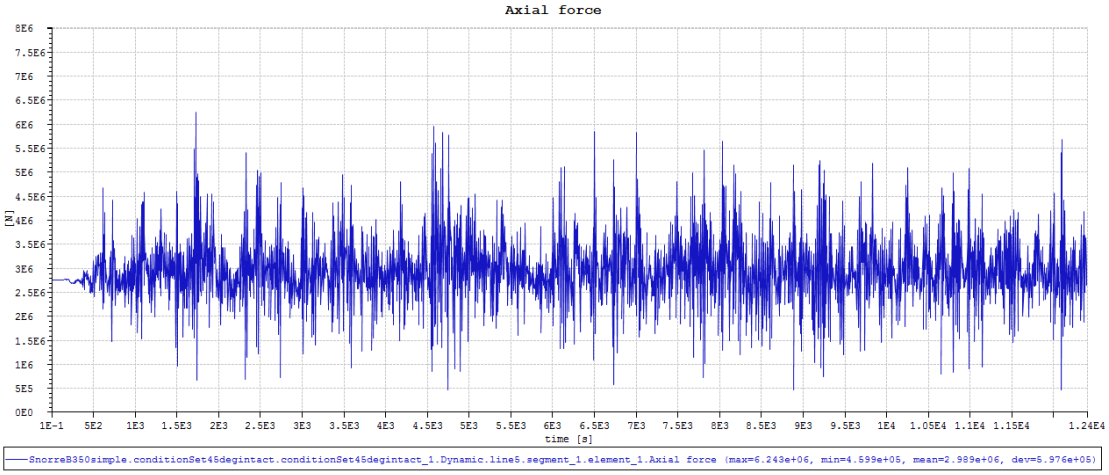

FIGURE 5.21: Time series of the tension in mooring line 5 for seed number 1

Chapter 6

Conclusion

Comparison of Time and Frequency Domain

The comparison of time and frequency domain shows that the methods are in deed comparable, but due to simplification and linearisation, the results are not identical. Especially the comparisons where the SIMO/RIFLEX signal has been filtered to give low frequency and wave frequency contributions, give large deviations. When the MIMOSA low frequency and wave frequency contributions are combined, the results are much better. Furthermore the deviation of max surge, mean, and max tension are acceptable. It is assumed that the non-linearities of the extreme environmental condition used for the comparison, further increase the deviations between the results, and that an analysis with intermediate sea state would yield even smaller deviations. The frequency domain software MIMOSA gives consistently conservative results, compared with the time domain software SIMO/RIFLEX. When choosing an analysis tool, one should carefully consider how prominent the non-linearities are, and make a decision based on the ratio of accuracy and computational cost.

Accidental Limit State Analysis

The analysis of accidental limit state shows that with one mooring line broken, the mean and max tension were increased by 21% and 25%, respectively. This means that the mooring system is robust against overload in the remaining lines. Given that the

minimum breaking strength (MBS) is 100% of expected, which is reasonable, there is only a 0.03% chance of failure of the second most loaded line. If the MBS is reduced to 80% capacity, there is still only a 1.38% chance of failure for the second most loaded line.

The analysis of the specific condition, shows that the tension peak does not occur for the transient phase after a line failure. Instead, the maximum tension recorded, is lowered, as the time of failure approaches the moment of the tension peak. This means that for the condition studied, ULS is the governing design criterion.

Chapter 7

Further Work

The problems with the taut-leg mooring system should naturally be resolved. This would create a better foundation for the comparison of frequency and time domain. As the taut-leg mooring system is entirely different from the catenary mooring system, and in a substantially larger water depth, this could give different results and lead to a different conclusion.

The methods could also be studied under a less severe sea state, where the non-linearities may not be so prominent. The deviations are then assumed to be smaller, since non-linearities have to be linearised in frequency domain, which doesn't always give acceptable results.

The ALS analysis should be further investigated, especially the time of failure. The condition analysed, with an extreme tension peak, suggests that the transient phase after a line failure, and subsequent tension peaks, are not governing. This is probably a special case due to the extreme tension peak, and probably not representative. A more general study should therefore be conducted, where the time of failure is analysed for other seed numbers.

Appendix A

SIMO and MIMOSA Plots

RAOs

Surge

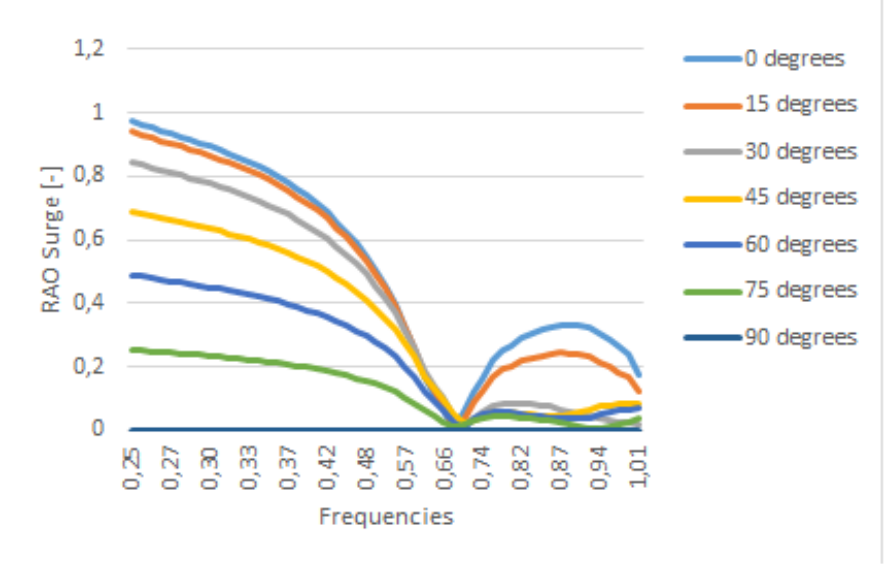

FIGURE A.1: RAO Surge SIMO

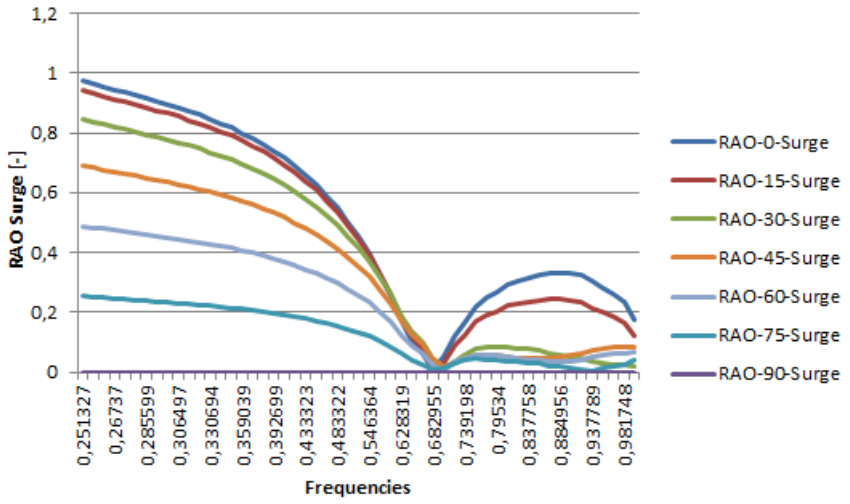

FIGURE A.2: RAO Surge MIMOSA

Sway

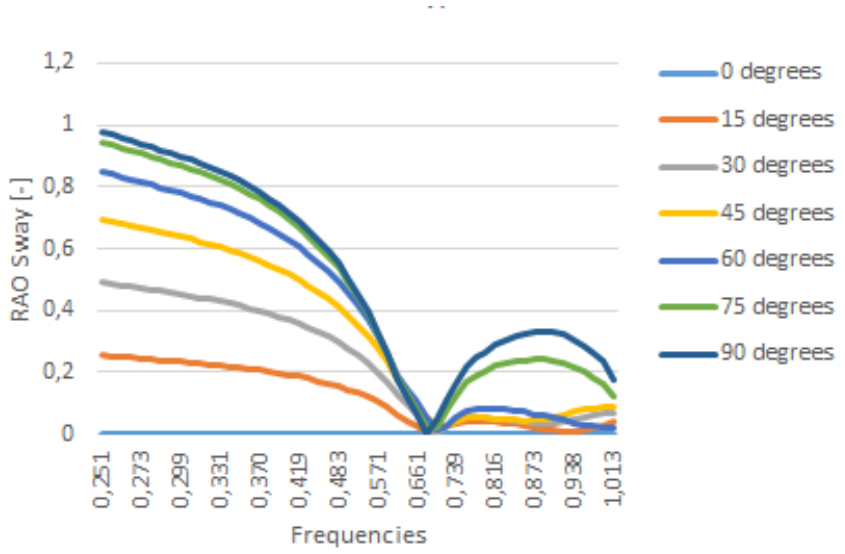

FIGURE A.3: RAO Sway SIMO

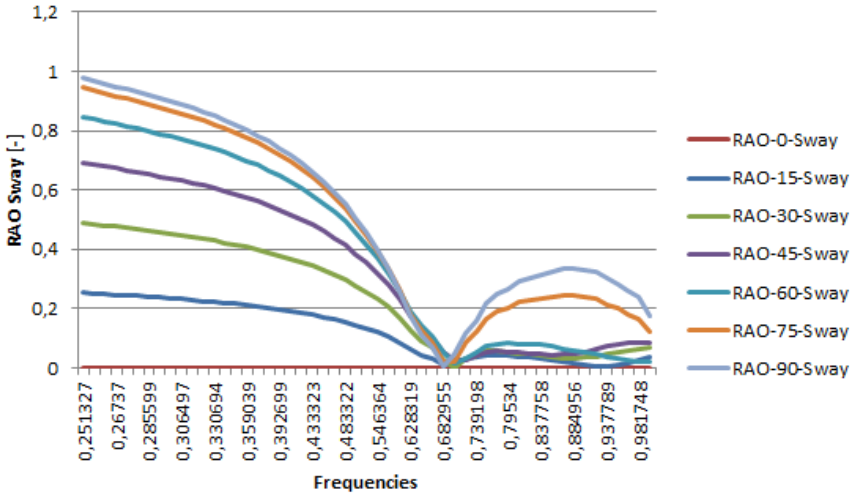

FIGURE A.4: RAO Sway MIMOSA

Heave

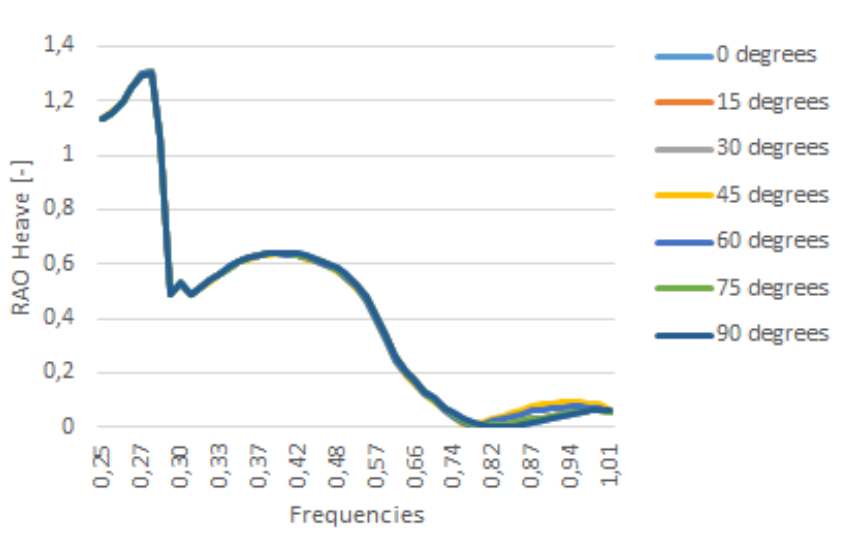

FIGURE A.5: RAO Heave SIMO

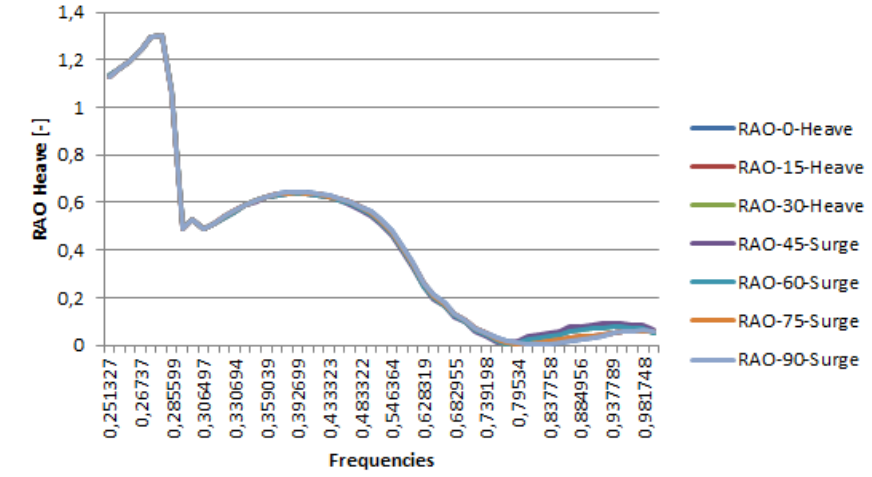

FIGURE A.6: RAO Heave MIMOSA

Roll

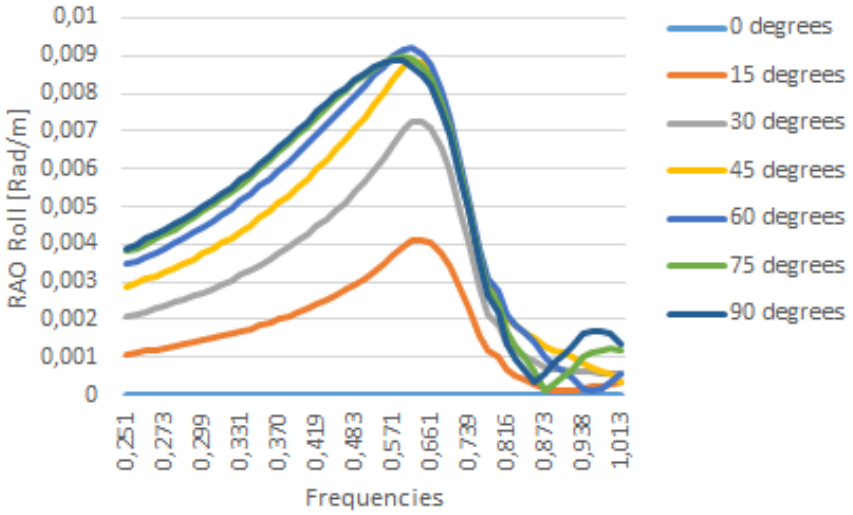

FIGURE A.7: RAO Roll SIMO

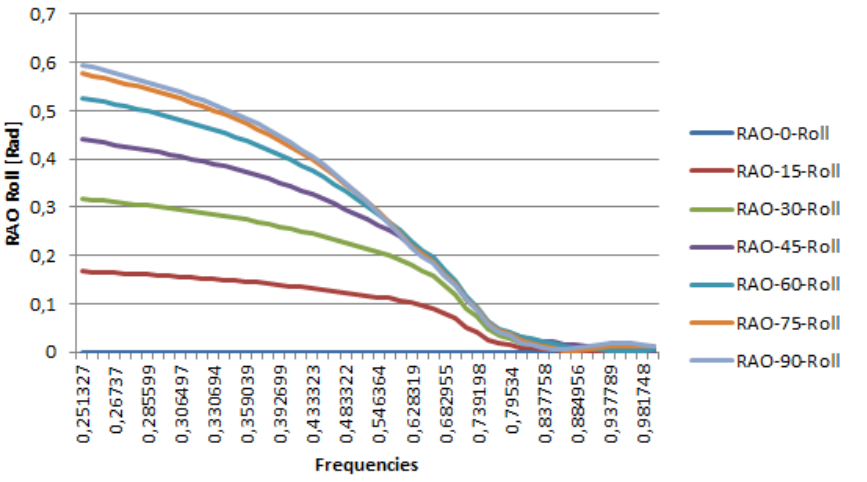

FIGURE A.8: RAO Roll MIMOSA

Pitch

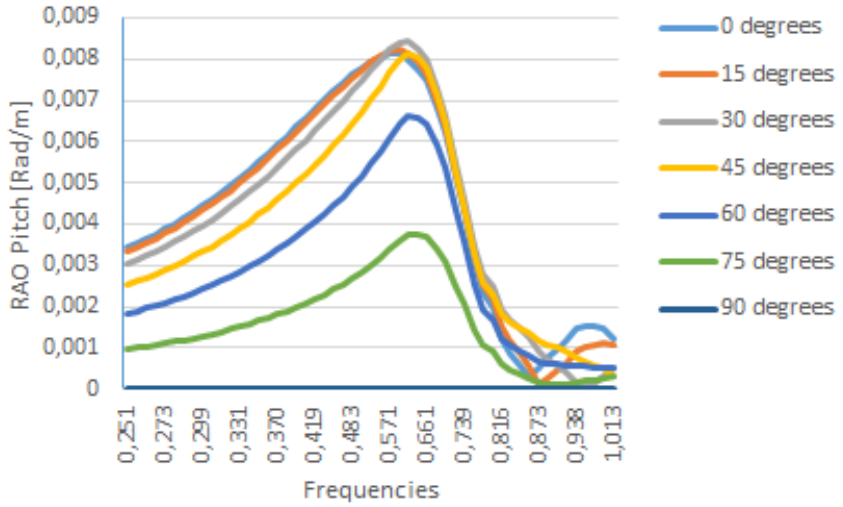

FIGURE A.9: RAO Pitch SIMO

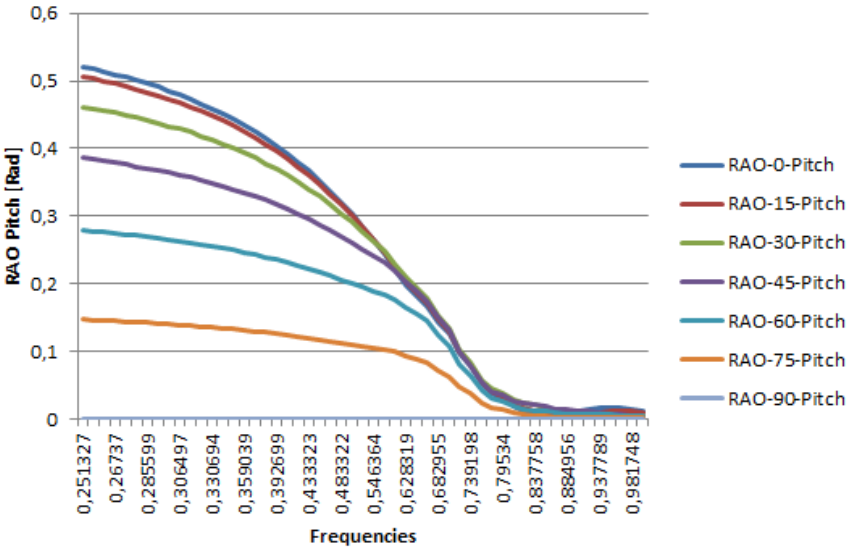

FIGURE A.10: RAO Pitch MIMOSA

Yaw

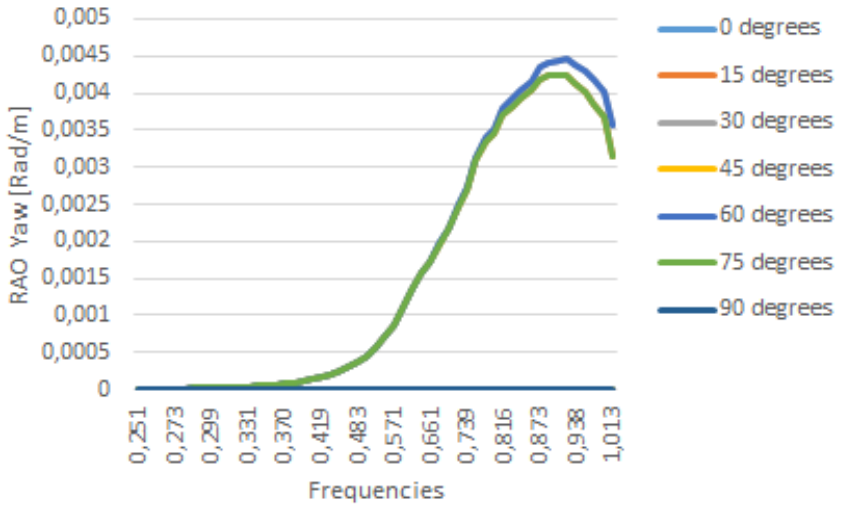

FIGURE A.11: RAO Yaw SIMO

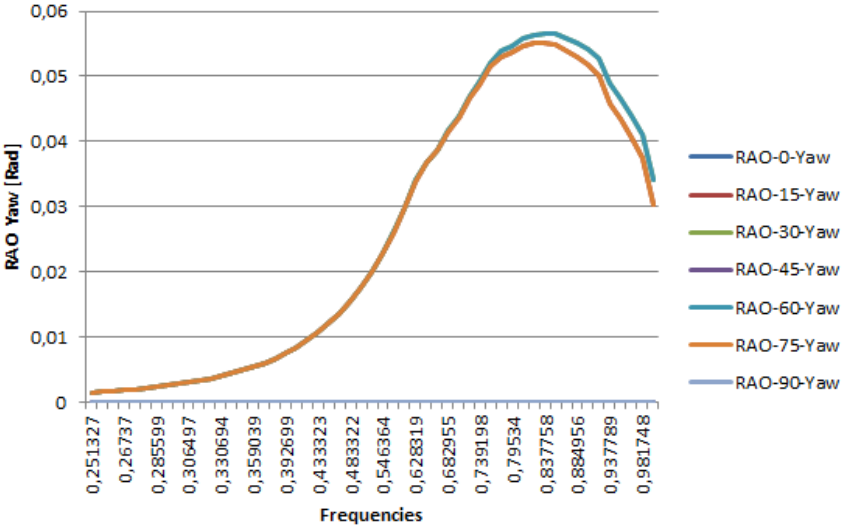

FIGURE A.12: RAO Yaw MIMOSA

Wind and Current Force Coefficients

Wind Force Coefficients

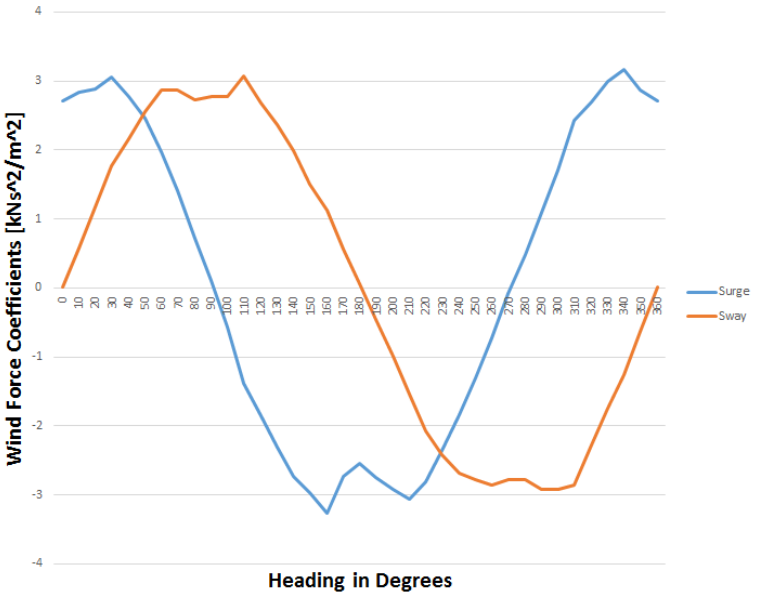

FIGURE A.13: Wind Force Coefficients SIMO

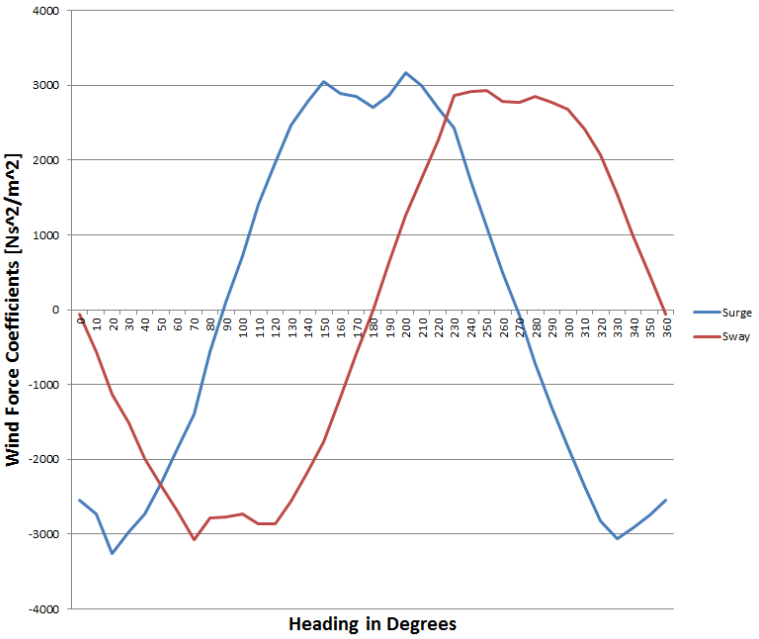

FIGURE A.14: Wind Force Coefficients MIMOSA

Current Force Coefficients

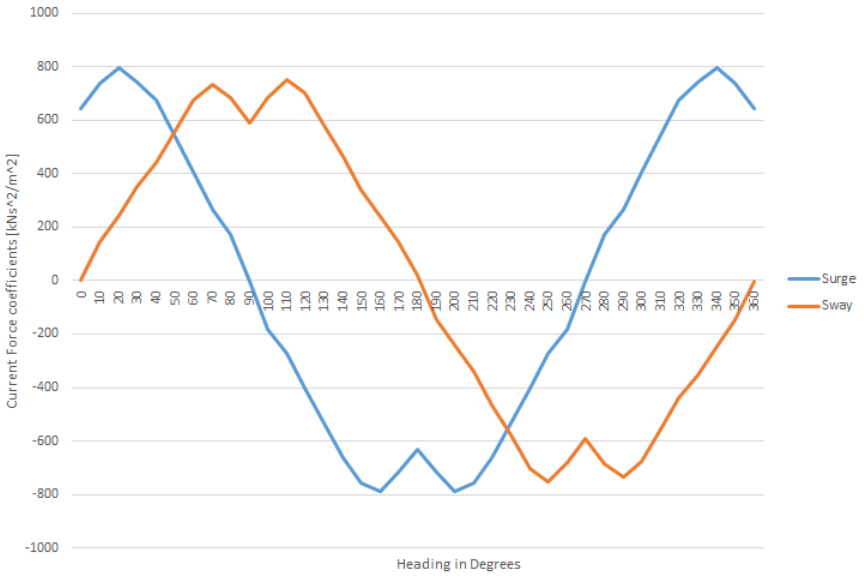

FIGURE A.15: Current Force Coefficients SIMO

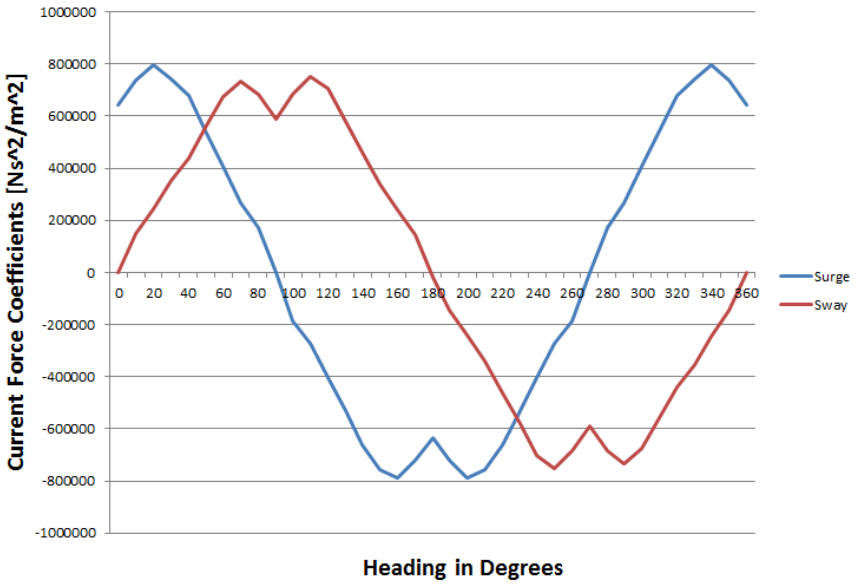

FIGURE A.16: Current Force Coefficients MIMOSA

Appendix B

Mooring Input Files

Catenary mooring system

```
'************************************************************************
 VESSEL POSITION
'************************************************************************
'chmoor
 SnorreB: 16 mooring lines - 1 characteristic
'x1ves     x2ves     x3ves     x6ves
 0.0000000 0.0000000 0.0000000 0.0000000
'------------------------------------------------------------------------
 LINE DATA
'iline lichar inilin iwirun intact
 1     1      1      0      1
'tpx1        tpx2
 40.2000000 44.5000000
'alfa         tens         xwinch
 37.5000000 1700.000000 0.0000000
'------------------------------------------------------------------------
 LINE DATA
'iline lichar inilin iwirun intact
 2     1      1      0      1
'tpx1        tpx2
 36.7000000 44.5000000
'alfa         tens         xwinch
 42.5000000 1700.8000000 0.0000000
'------------------------------------------------------------------------
 LINE DATA
'iline lichar inilin iwirun intact
 3     1      1      0      1
'tpx1        tpx2
 33.2000000 44.5000000
'alfa         tens         xwinch
 47.5000000 1700.000000 0.0000000
'------------------------------------------------------------------------
 LINE DATA
'iline lichar inilin iwirun intact
 4     1      1      0      1
'tpx1        tpx2
 29.7000000 44.5000000
'alfa         tens         xwinch
 52.5000000 1700.6000000 0.0000000
'------------------------------------------------------------------------
 LINE DATA
'iline lichar inilin iwirun intact
 5     1      1      0      1
'tpx1       tpx2
 -29.7000000 44.5000000
'alfa        tens        xwinch
 127.5000000 1700.000000 0.0000000
'------------------------------------------------------------------------
 LINE DATA
'iline lichar inilin iwirun intact
 6     1      1      0      1
'tpx1       tpx2
 -33.2000000 44.5000000
'alfa        tens        xwinch
 132.5000000 1700.000000 0.0000000
'------------------------------------------------------------------------
 LINE DATA
'iline lichar inilin iwirun intact
 7     1      1      0      1
'tpx1       tpx2
 -36.7000000 44.5000000
'alfa        tens        xwinch
 137.5000000 1700.0000000 0.0000000
'------------------------------------------------------------------------
 LINE DATA
'iline lichar inilin iwirun intact
 8     1      1      0      1
'tpx1       tpx2
 -40.2000000 44.5000000
'alfa        tens        xwinch
```

```
 142.500000 1700.000000 0.0000000
'------------------------------------------------------------------------
 LINE DATA
'iline lichar inilin iwirun intact
 9     1      1      0      1
'tpx1       tpx2
 -40.2000000 -44.5000000
'alfa       tens        xwinch
 217.5000000 1700.0000000 0.0000000
'------------------------------------------------------------------------
 LINE DATA
'iline lichar inilin iwirun intact
 10    1     1      0      1
'tpx1       tpx2
 -36.7000000 -44.5000000
'alfa       tens        xwinch
 222.500000 1700.000000 0.0000000
'------------------------------------------------------------------------
 LINE DATA
'iline lichar inilin iwirun intact
 11    1     1      0      1
'tpx1       tpx2
 -33.2000000 -44.5000000
'alfa       tens        xwinch
 227.5000000 1700.000000 0.0000000
'------------------------------------------------------------------------
 LINE DATA
'iline lichar inilin iwirun intact
 12    1     1      0      1
'tpx1       tpx2
 -29.7000000 -44.5000000
'alfa       tens        xwinch
 232.5000000 1700.000000 0.0000000
'------------------------------------------------------------------------
 LINE DATA
'iline lichar inilin iwirun intact
 13    1     1      0      1
'tpx1        tpx2
 29.7000000 -44.5000000
'alfa        tens         xwinch
 307.500000 1700.000000 0.0000000
'------------------------------------------------------------------------
 LINE DATA
'iline lichar inilin iwirun intact
 14    1     1      0      1
'tpx1        tpx2
 33.2000000 -44.5000000
'alfa        tens         xwinch
 312.5000000 1700.000000 0.0000000
'------------------------------------------------------------------------
 LINE DATA
'iline lichar inilin iwirun intact
 15    1     1      0      1
'tpx1        tpx2
 36.7000000 -44.5000000
'alfa        tens         xwinch
 317.5000000 1700.000000 0.0000000
'------------------------------------------------------------------------
 LINE DATA
'iline lichar inilin iwirun intact
 16    1     1      0      1
'tpx1        tpx2
 40.2000000 -44.5000000
'alfa        tens         xwinch
 322.5000000 1700.000000 0.0000000
'------------------------------------------------------------------------
 '-----------------------------------------------------------------------
 LINE CHARACTERISTICS DATA
'lichar
 1
'linpty npocha npv
 2      20     2
'nseg ibotco icurli
 4    1      0
'anbot     tpx3       x3ganc      tmax          fric
 0.0000000 12.6000000 350.0000000 15357.0000000 0.6000000
```

```
'iseg ieltyp nel ibuoy sleng       nea brkstr
 1    0      80  0     800.0000000 1   16992.0000000
 2    0      60  0     285.0000000 1   25000.0000000
 3    0      30  0     25.0000000 1   16992.0000000
 4    0      90  0     92.9000000 1   18665.0000000
'iseg dia       emod          emfact    uwiw      watfac    cdn       cdl
 1    0.1370000 3.9000000e+07 2.0000000 3.2440956 0.8490834 2.7503650 1.3178832
 2    0.1480000 9.0700000e+07 1.0000000 0.6883521 0.7542261 1.3621622 0.1135135
 3    0.1370000 3.9000000e+07 2.0000000 3.2604605 0.8029263 3.4510949 1.6536496
 4    0.1450000 3.6900000e+07 2.0000000 3.8524444 0.7449789 4.3862069 2.1017241
'-------------------------------------------------------------------------
END
```

Taut-leg mooring system

```
'************************************************************************
 VESSEL POSITION
'************************************************************************
'chmoor
 SnorreB: 16 mooring lines - 1 characteristic
'x1ves     x2ves     x3ves     x6ves
 0.0000000 0.0000000 0.0000000 0.0000000
'------------------------------------------------------------------------
 LINE DATA
'iline lichar inilin iwirun intact
 1     1      1      0      1
'tpx1        tpx2
 40.2000000 44.5000000
'alfa         tens         xwinch
 37.5000000 1700.000000 0.0000000
'------------------------------------------------------------------------
 LINE DATA
'iline lichar inilin iwirun intact
 2     1      1      0      1
'tpx1        tpx2
 36.7000000 44.5000000
'alfa         tens         xwinch
 42.5000000 1700.8000000 0.0000000
'------------------------------------------------------------------------
 LINE DATA
'iline lichar inilin iwirun intact
 3     1      1      0      1
'tpx1        tpx2
 33.2000000 44.5000000
'alfa         tens         xwinch
 47.5000000 1700.000000 0.0000000
'------------------------------------------------------------------------
 LINE DATA
'iline lichar inilin iwirun intact
 4     1      1      0      1
'tpx1        tpx2
 29.7000000 44.5000000
'alfa         tens         xwinch
 52.5000000 1700.6000000 0.0000000
'------------------------------------------------------------------------
 LINE DATA
'iline lichar inilin iwirun intact
 5     1      1      0      1
'tpx1       tpx2
 -29.7000000 44.5000000
'alfa        tens        xwinch
 127.5000000 1700.000000 0.0000000
'------------------------------------------------------------------------
 LINE DATA
'iline lichar inilin iwirun intact
 6     1      1      0      1
'tpx1       tpx2
 -33.2000000 44.5000000
'alfa        tens        xwinch
 132.5000000 1700.000000 0.0000000
'------------------------------------------------------------------------
 LINE DATA
'iline lichar inilin iwirun intact
 7     1      1      0      1
'tpx1       tpx2
 -36.7000000 44.5000000
'alfa        tens        xwinch
 137.5000000 1700.0000000 0.0000000
'------------------------------------------------------------------------
 LINE DATA
'iline lichar inilin iwirun intact
 8     1      1      0      1
'tpx1       tpx2
 -40.2000000 44.5000000
'alfa        tens        xwinch
 142.500000 1700.000000 0.0000000
```

```
'-------------------------------------------------------------------------
 LINE DATA
'iline lichar inilin iwirun intact
 9     1      1      0      1
'tpx1       tpx2
 -40.2000000 -44.5000000
'alfa       tens        xwinch
 217.5000000 1700.0000000 0.0000000
'-------------------------------------------------------------------------
 LINE DATA
'iline lichar inilin iwirun intact
 10    1     1      0      1
'tpx1       tpx2
 -36.7000000 -44.5000000
'alfa       tens        xwinch
 222.500000 1700.000000 0.0000000
'-------------------------------------------------------------------------
 LINE DATA
'iline lichar inilin iwirun intact
 11    1     1      0      1
'tpx1       tpx2
 -33.2000000 -44.5000000
'alfa       tens        xwinch
 227.5000000 1700.000000 0.0000000
'-------------------------------------------------------------------------
 LINE DATA
'iline lichar inilin iwirun intact
 12    1     1      0      1
'tpx1       tpx2
 -29.7000000 -44.5000000
'alfa       tens        xwinch
 232.5000000 1700.000000 0.0000000
'-------------------------------------------------------------------------
 LINE DATA
'iline lichar inilin iwirun intact
 13    1     1      0      1
'tpx1        tpx2
 29.7000000 -44.5000000
'alfa        tens         xwinch
 307.500000 1700.000000 0.0000000
'-------------------------------------------------------------------------
 LINE DATA
'iline lichar inilin iwirun intact
 14    1     1      0      1
'tpx1        tpx2
 33.2000000 -44.5000000
'alfa        tens         xwinch
 312.5000000 1700.000000 0.0000000
'-------------------------------------------------------------------------
 LINE DATA
'iline lichar inilin iwirun intact
 15    1     1      0      1
'tpx1        tpx2
 36.7000000 -44.5000000
'alfa        tens         xwinch
 317.5000000 1700.000000 0.0000000
'-------------------------------------------------------------------------
 LINE DATA
'iline lichar inilin iwirun intact
 16    1     1      0      1
'tpx1        tpx2
 40.2000000 -44.5000000
'alfa        tens         xwinch
 322.5000000 1700.000000 0.0000000
'-------------------------------------------------------------------------
 '------------------------------------------------------------------------
 LINE CHARACTERISTICS DATA
'lichar
 1
'linpty npocha npv
 2      20     2
'nseg ibotco icurli
 3    1      0
'anbot     tpx3       x3ganc      tmax          fric
 0.0000000 12.6000000 1500.0000000 18639.0000000 0.6000000
'iseg ieltyp nel ibuoy sleng       nea brkstr
```

```
 1    0      80  0     100.0000000 1   18665.0000000
 2    0      200  0     1922.0000000 1   18639.0000000
 3    0      80  0     100.0000000 1   18665.0000000
'iseg dia       emod          emfact    uwiw      watfac    cdn       cdl
 1    0.1450000 3.6900000e+07 2.0000000 3.587 0.87 2.6 0.0
 2    0.2630000 5.0856000e+06 1.0000000 0.1089 0.25 1.6 0.0
 3    0.1450000 3.6900000e+07 2.0000000 3.587 0.87 2.6 0.0
'-------------------------------------------------------------------------
END
```

Appendix C

Overview of Attached Files

posterportrait.pfd

posterportrait.pfd is the poster for the poster exhibition.

moor.txt

moor.txt is the catenary mooring input file. The file can also be seen in Appendix B.

moor1500lea.txt

moor1500.txt is the taut-leg mooring input file. The model wasn't properly imported to RIFLEX, so no results are attained from the file, but it is attached only as a documentation.The file can also be seen in Appendix B.

vessel.mos

vessel.mos is the vessel file used for both mooring systems.

mastersima.stask

mastersima.stask is the SIMA workspace, containing the SIMA models and post-processors. All the results from SIMO/RIFLEX can be recreated by running this file.

Bibliography

Brindley, W. and Brandsæter, A.

2015. Empirical probability of one and two line failures.

DNV GL

2004. Metocean design basis.

DNV GL

2013. *Position mooring*. DNV GL.

Faltinsen, O.

1990. *Sea Loads on Ships and Offshore Structures*. Cambridge University Press.

ISO Standard

2013. *Petroleum and natural gas industries - Specific requirements for offshore structures*. Part 7: Stationkeeping systems for floating offshore structures and mobile offshore units.

Kwan, C.

1991. Design practice for mooring of floating production systems. *Marine Technology*.

Larsen, C.M.

2012. *Marine Dynamics*. Department of Marine Technology.

Larsen, K.

2014a. Lecture notes tmr4225 marine operations, NTNU.

Larsen, K.

2014b. Static equilibrium of a mooring line.

Larsen, K.

2015. Personal communication.

Leira, B.

2010. *Lecture Notes, TMR4235 Stochastic Theory of Sealoads*. Department of marine technology, NTNU.

Lie, H., Gao, Z., and Moan, T.

2007. Mooring line damping estimation by a simplified dynamic model. *OMAE2007-29155*.

Løken, A.E., Sødahl, N., and Hagen, Ø.

1999. Efficient integrated analysis methods for deepwater platforms. *OTC 10809*.

Marintek

2009. *SIMO Theory Manual*.

Marintek

2012. Mimosa user's documentation.

Marintek

2014. *RIFLEX Theory Manual*.

Næss, A. and Moan, T.

2013. *Stochastic Dynamics of Marine Structures*. Cambridge University Press.

Ormberg, H. and Larsen, K.

2004. Coupled analysis of floater motion and mooring dynamics for a turret-moored ship. *Applied Ocean Research*.

Statoil

2001. *Snorre B Operation Manual*

Stendal, L.C.

2014. Mooring of floating vessels in deep waters. Project thesis fall 2014.